Supplementary Information

Addressable DNA nanotubes with repetitive components

Tanxi Bai, Bryan Wei*

School of Life Sciences, Tsinghua University-Peking University Center for Life Sciences, Center for Synthetic and Systems Biology, Tsinghua University, Beijing 100084, China

*Correspondences and requests for materials should be addressed to B.W. (email: bw@tsinghua.edu.cn)

This PDF file includes:

DNA sequence design

Structures shown in this study were adapted from previous studies[1,2]. All the structures were designed by sequence generation software Uniquimer[3]. DNA sequences can be found in Supplementary Information 2.

Structural assembly

DNA oligonucleotides without modification were synthesized by Integrated DNA Technology Incorporation, Bioneer Corporation or Sangon Biotech Corporation and were used without further purifications. To assemble tubular structures with different numbers of addressable helices, component strands were mixed at a roughly equal molar final concentration of 100-1200 nM per strand, in 0.5 × TE buffer (5 mM Tris, pH = 7.9 and 1 mM EDTA) or 1 × TAE buffer (40 mM Tris, pH = 8.0, 20 mM acetic acid and 1 mM EDTA), supplemented with 15-20 mM $MgCl_2$. The DNA mixture was then annealed with a 'ramp' annealing program cooling down from 85 °C to 10 °C over a course of 24 h. To assemble tubular structures from two addressable rows of U-SSTs with 10 to 100 columns, component strands were annealed at 45 °C for 40 hours.

Gel electrophoresis and yield quantification

Annealed samples were subjected to 2.5% native agarose gel electrophoresis in an ice-water bath, and gels were prepared in 0.5 × TBE buffer (44.5 mM Tris, 44.5 mM boric acid, and 1 mM EDTA) with 10 mM $MgCl_2$ and pre-stained with SYBR Safe (Thermo Fisher Scientific). To purify desired structures, target bands were excised and finely crushed in a Freeze'N Squeeze column (Bio-Rad), and then directly subjected to centrifugation at 438 × g for 3 min at 4 °C. Samples centrifuged through the column were collected for further analysis by TEM.

To quantify the assembly yield, the intensity of the target band was compared against a standard band[1] (e.g., 1500-base-pair band from a 1-kb DNA ladder mixture). The mass value of the target band was deduced from the intensity-mass correlation based on the standard band, and was used to calculate the yield of the desired structure.

Gold nanoparticle decoration

DNA strands with 3' thiol modification were purchased from Bioneer Corporation with HPLC purification. Phosphination of AuNPs and conjugation of thiolated DNA on to 5-nm and 10-nm Au were achieved following previous reported protocols[4-6]. In a typical experiment, the thiolated DNA strand was incubated with AuNPs capped with phosphine (2.5 mM) in a ratio of 100:1 in 0.5 × TBE containing 50 mM NaCl at room temperature for 36 hours in the dark. After that, NaCl was slowly added into the reaction solution to reach a final concentration of 0.2 M NaCl. DNA-AuNP conjugates were collected by Millipore Microcon (MWCO 100K, Billerica, MA). Purified tubular structures were mixed with DNA-AuNP conjugates and annealed from 37 °C to 20 °C over a course of 2 hours before imaging.

TEM imaging

A 3.5 μL droplet of sample was applied to a plasma-treated, carbon-coated grid (Electron Microscopy Sciences) for 2 min and then wicked off and stained for 60 s with 3.5 μL of stain buffer (2% aqueous uranyl acetate). Then stain buffer was blotted off by filter paper and left on the grid to be air-dried. The stained sample was analyzed by FEI Tecnai, operated at 200 kV at 29,000 to 50,000 magnification.

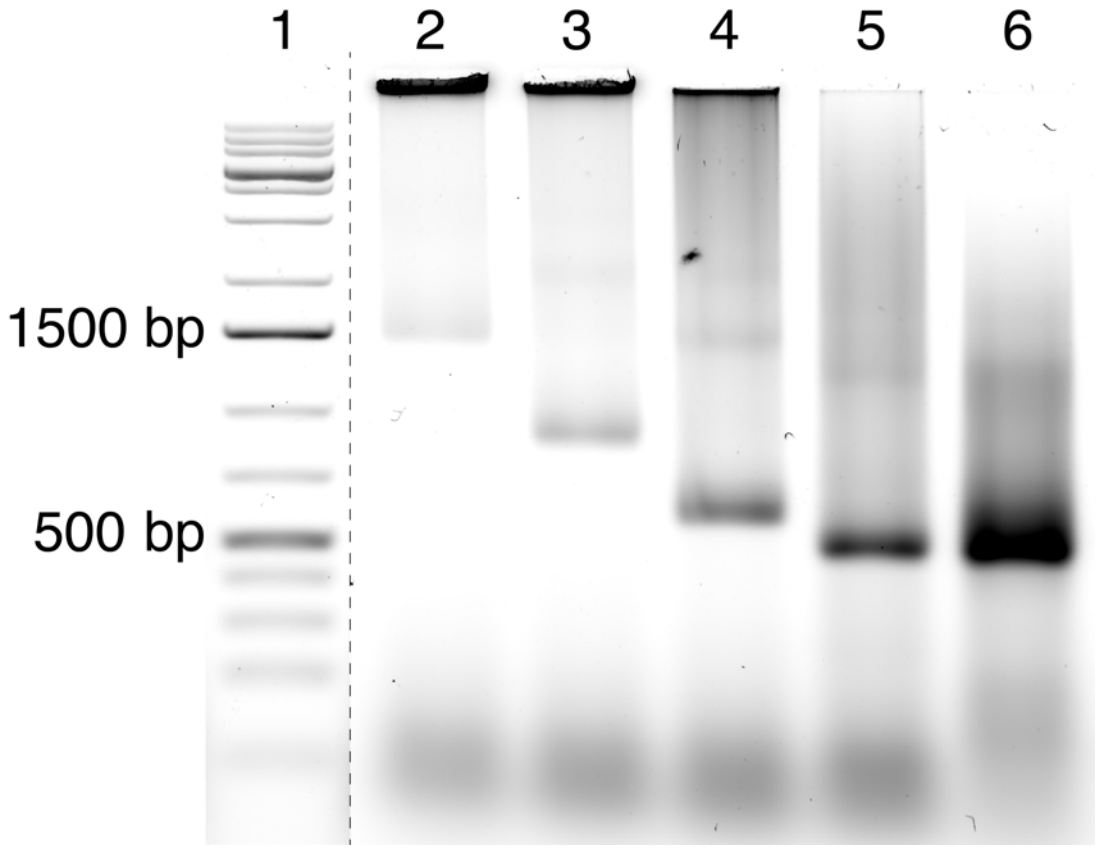

Figure S1. AGE results of tubes from different numbers of canonical SST rows as cyclization units. Lane 1: 1-kb ladder. Lane 2-6: Tubes from 24, 12, 6, 4 and 2 addressable rows of U-SSTs as cyclization units respectively. Discrete bands with incrementally increasing mobility correspond to the varying circumferences of the tube designs. The band in lane 6 (2-row cyclization units) shares the same mobility with the one in lane 5 (4-row cyclization units), which indicates that the resulted product corresponds to a 4-helix tube (multimerizing at 2×). Corresponding TEM images of unpurified products are shown in Figures S2-S6.

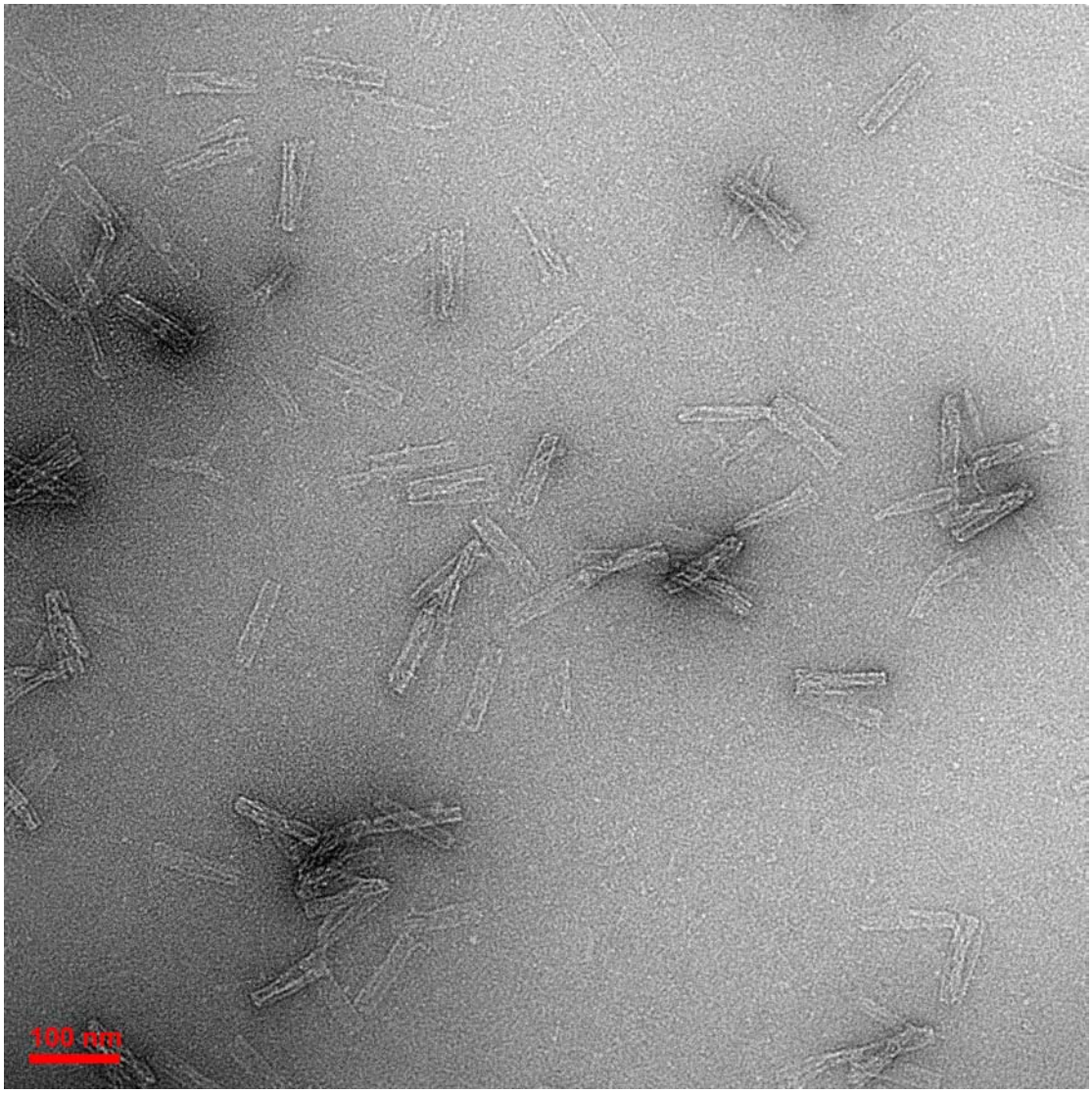

Figure S2. TEM image of tubes from the 24-row cyclization unit of U-SSTs directly after self-assembly without purification. Scale bar: 100 nm. Width measurements are shown in Table S1.

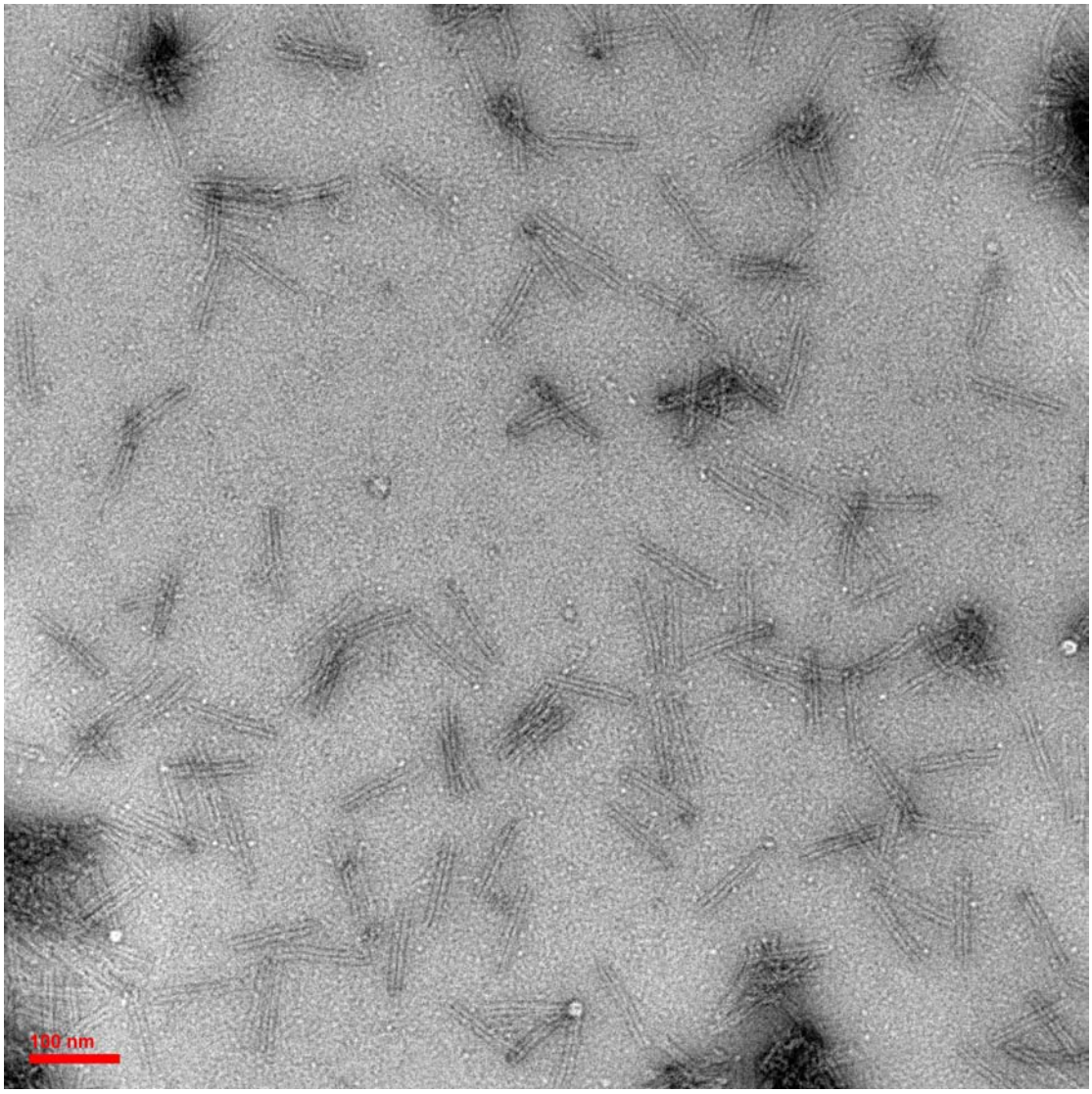

Figure S3. TEM image of tubes from the 12-row cyclization unit of U-SSTs directly after self-assembly without purification. Scale bar: 100 nm. Width measurements are shown in Table S1.

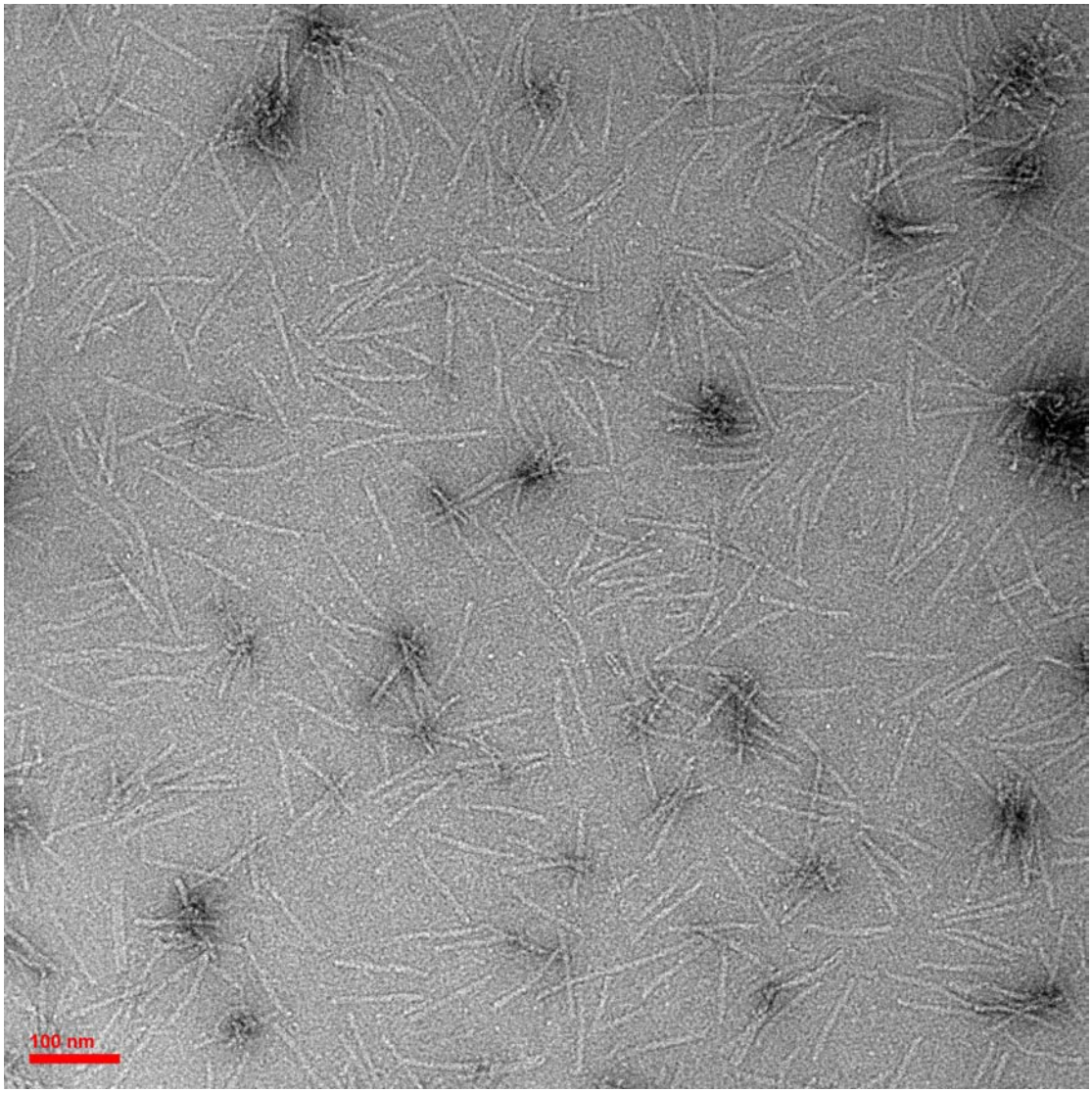

Figure S4. TEM image of tubes from the 6-row cyclization unit of U-SSTs directly after self-assembly without purification. Scale bar: 100 nm. Width measurements are shown in Table S1.

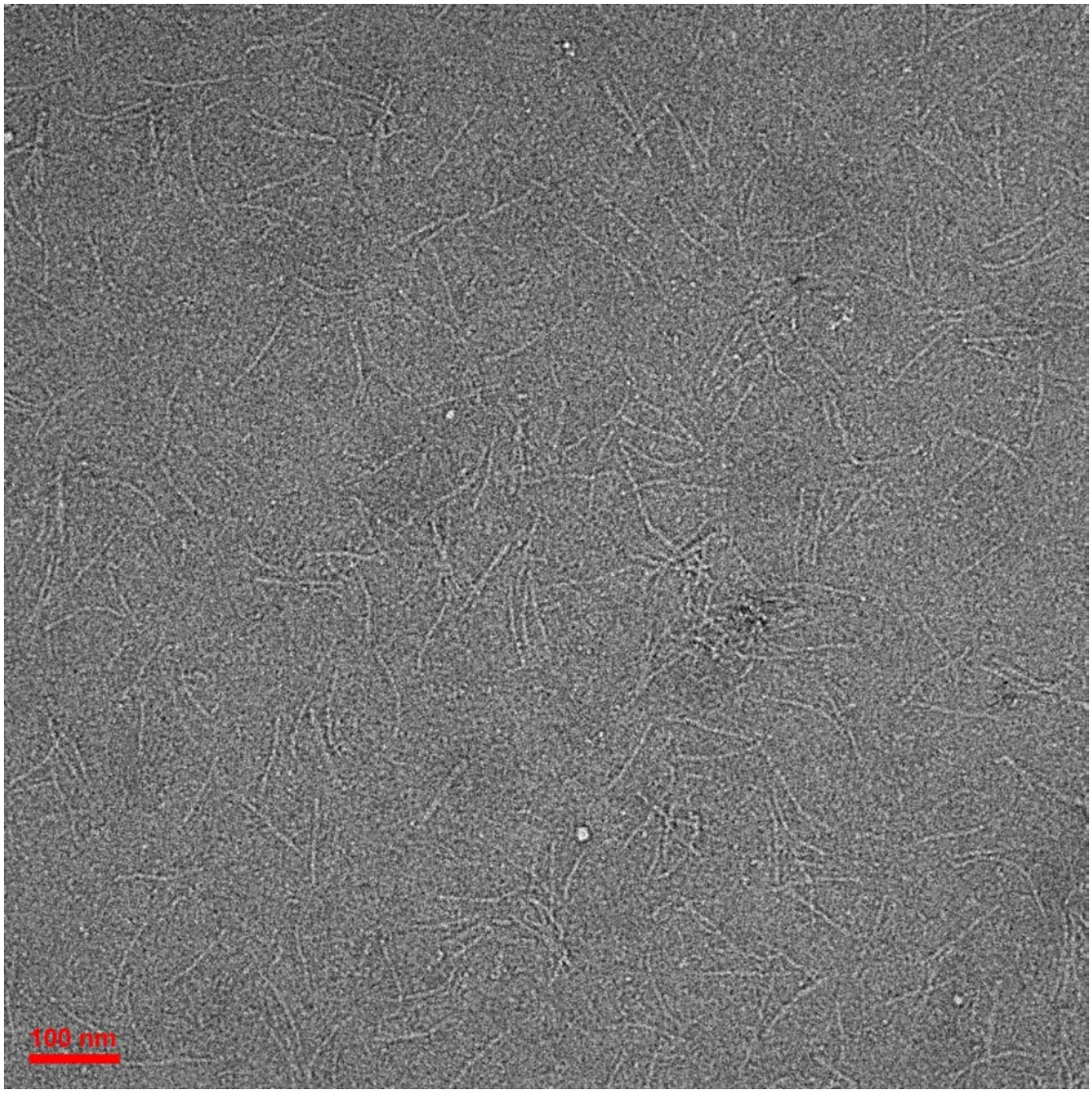

Figure S5. TEM image of tubes from the 4-row cyclization unit of U-SSTs directly after self-assembly without purification. Scale bar: 100 nm. Width measurements are shown in Table S1.

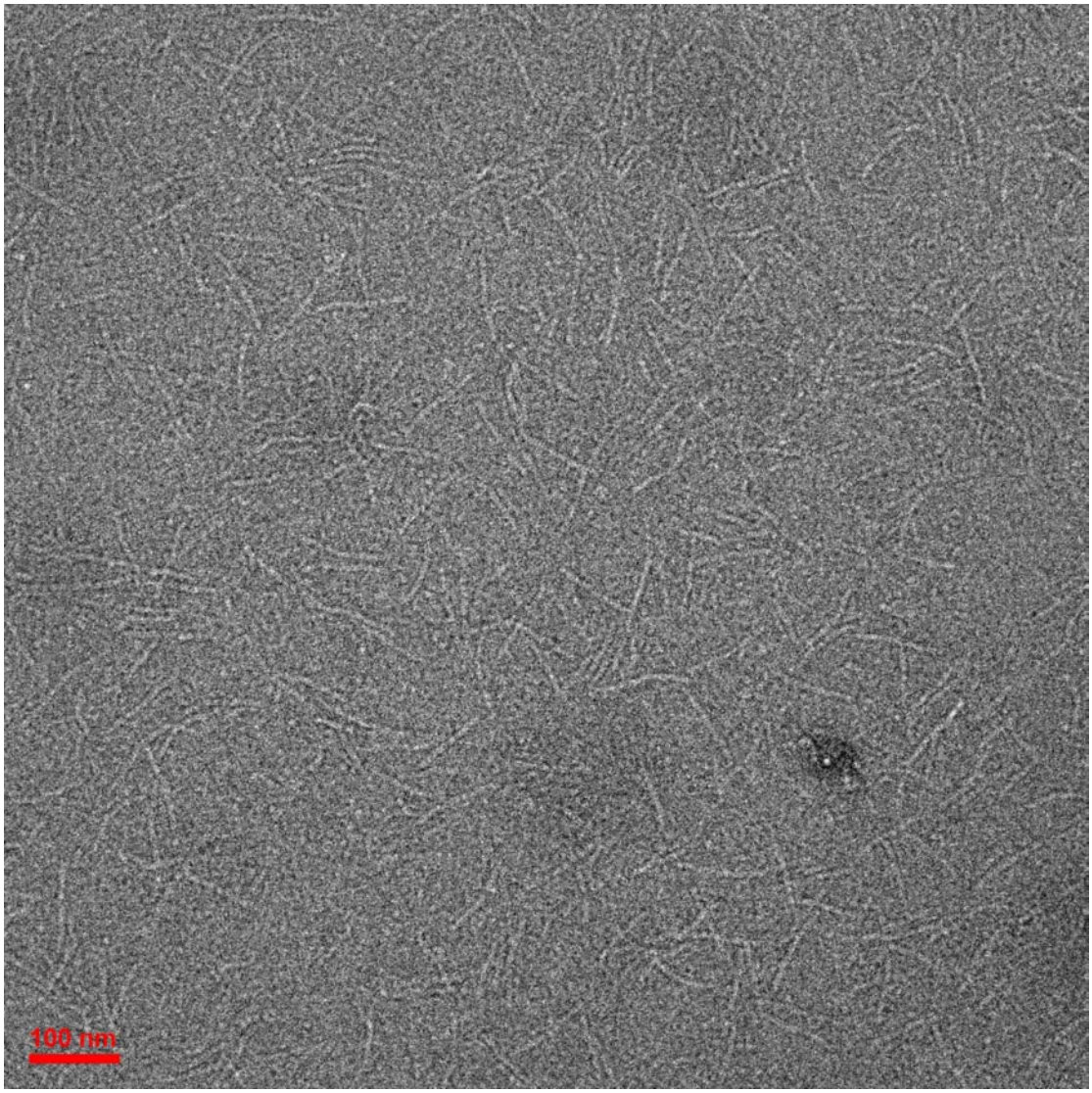

Figure S6. TEM image of tubes from the 2-row cyclization unit of U-SSTs directly after self-assembly without purification. Scale bar: 100 nm. Width measurements are shown in Table S1.

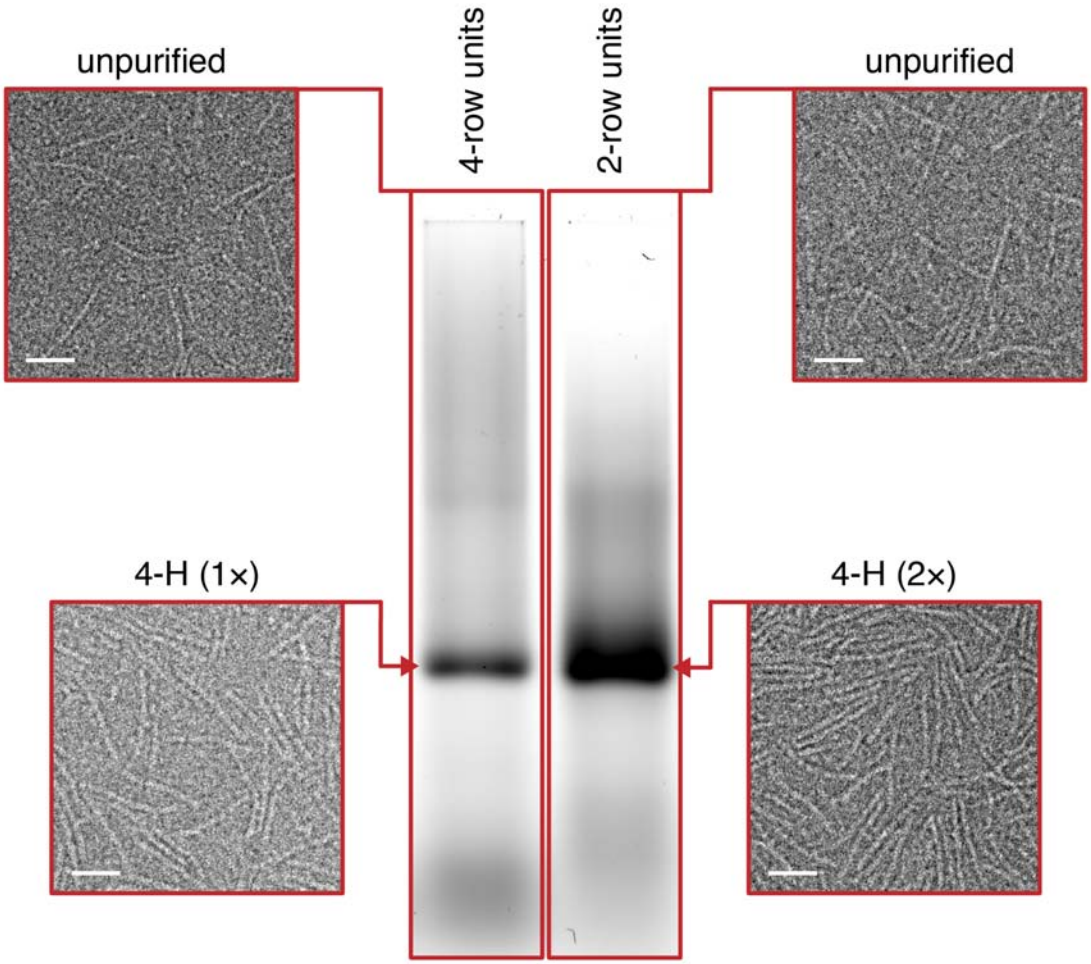

Figure S7. AGE and TEM results of the 4-row and 2-row cyclization units of U-SSTs. AGE results are shown in the middle. Monodisperse products of 4-row and 2-row cyclization units are pointed by triangles. The rectangles framing the whole lane depict the products after self-assembly without purification. Corresponding TEM images of 4-row and 2-row cyclization units are presented on the left and right respectively. Scale bars: 50 nm.

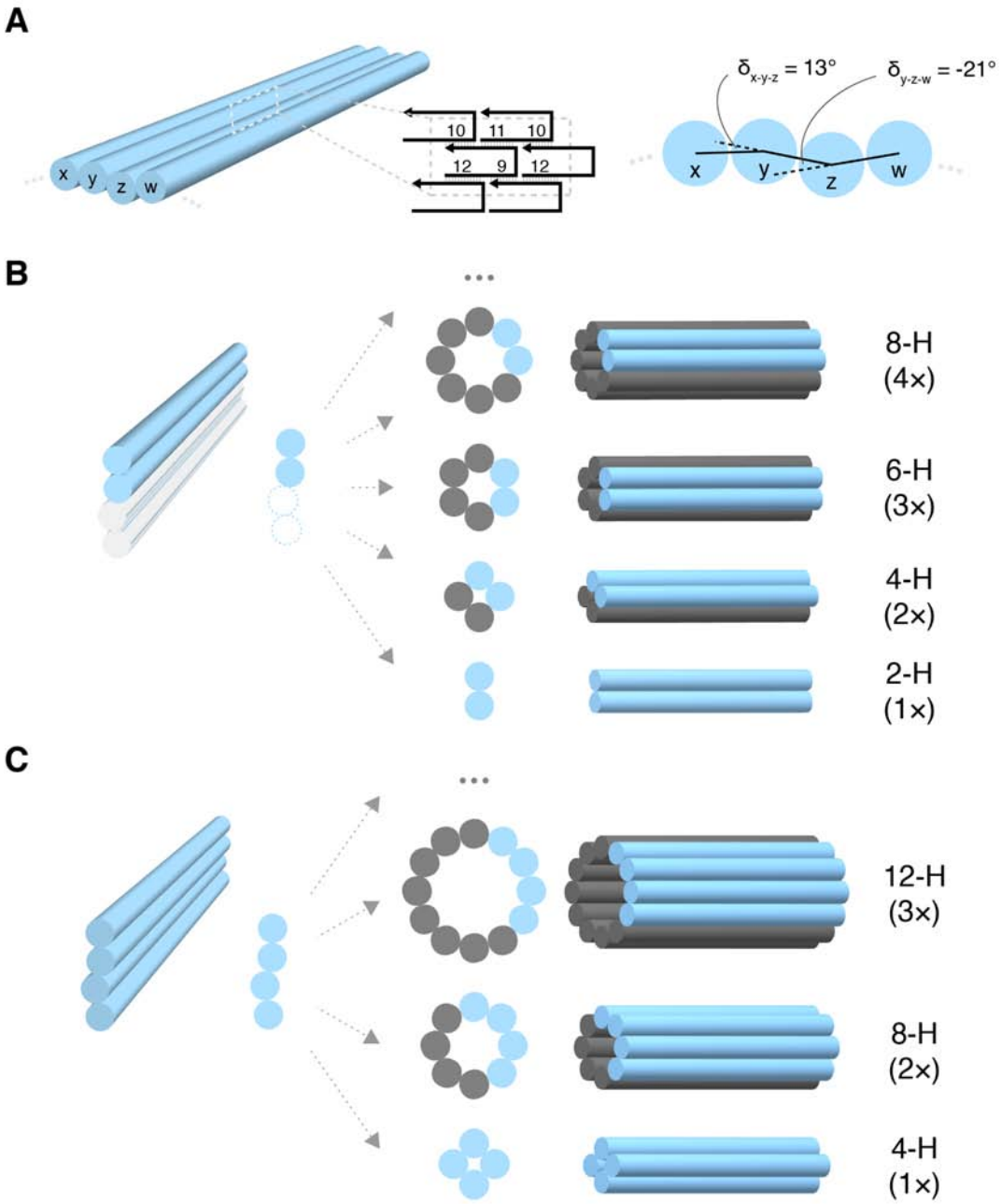

Figure S8. Tubulation of U2-SSTs. (**A**) Schematics of tube curvature accumulation with U2-SSTs. Left: cylinder diagram of a monolayer structure and a zoomed-in section highlights SSTs with specific strand specifications (numbers indicate the domain length in nucleotide); right: along-axis view (calculation of dihedral angles and curvatures based on the previous study)[2]. A curvature (δ) is the supplementary angle of a dihedral angle formed by three adjacent helices (i.e., x, y and z) and the average curvature (average of $\delta_{x\text{-}y\text{-}z}$ and $\delta_{y\text{-}z\text{-}w}$) is -4° (average of 13° and -21°). (**B, C**) Schematics of the 2-row (**B**) and 4-row (**C**) cyclization units and the tubulation tendencies. Left: cylinder diagrams and along-axis views of the cyclization units. Virtual cylinders (in pale white with dashed outline) are provided to better illustrate the dihedral angle and curvature. Right: different tubulation tendencies of the cyclization units and resulted products with multiple levels of repetition (e.g., 2-row units forming monomer products or multimerizing at 2×, 3×, 4× as 4-H, 6-H, 8-H tubes). A repeating cyclization unit is highlighted in cyan for each design.

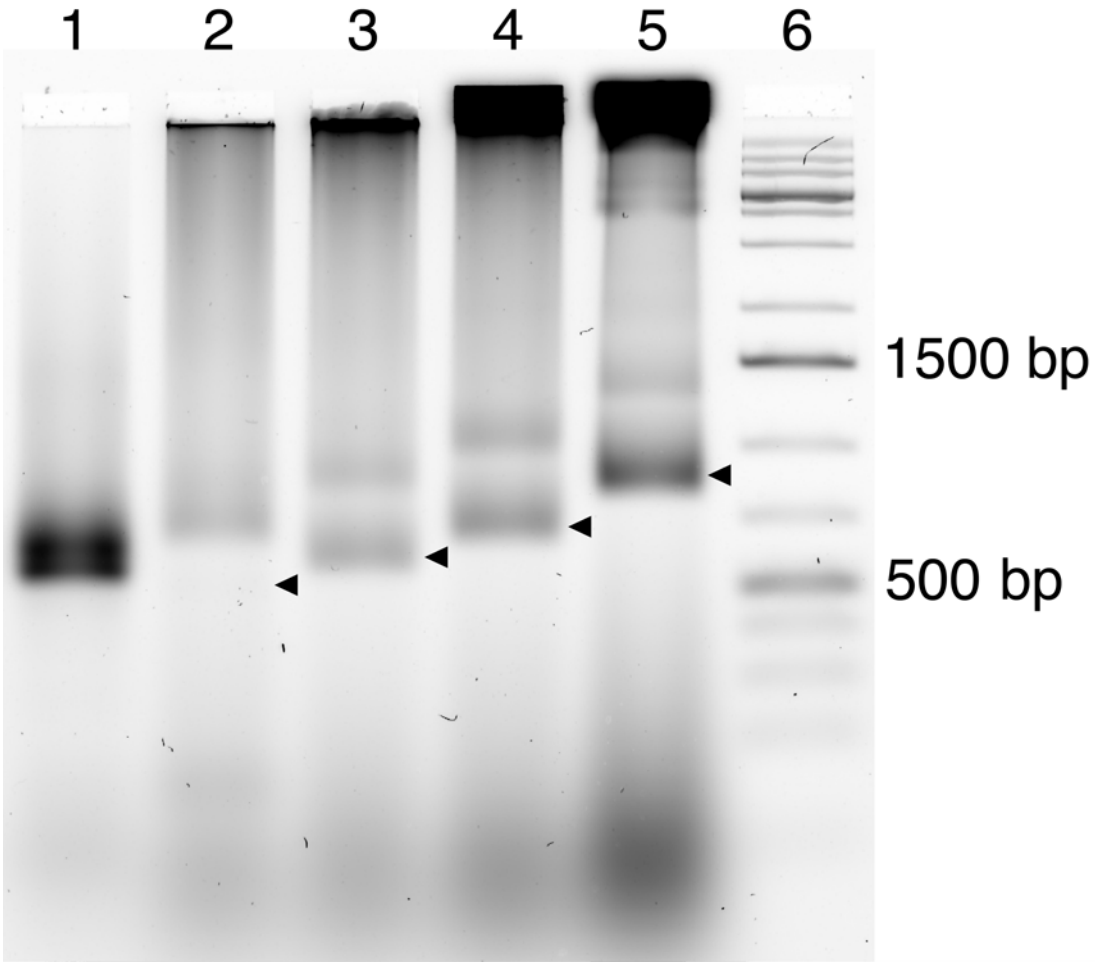

Figure S9. AGE results of tubes from different numbers of U2-SST rows as cyclization units. Lane 1-5: Tubes from 2, 4, 6, 8 and 12 addressable rows of U2-SSTs as cyclization units respectively. A series of bands in each lane correspond to multiple repetitive levels of a cyclization unit (1×, 2×, 3×, etc.). The monomer bands (1×) in each lane are pointed by triangles. Specifically, no monomer band is available in lane 1 and the lowest band in lane 1 ran slower than the monomer band in lane 2 (4-row cyclization units at 1×), indicating the resulted product of the 2-row cyclization unit multimerizes at 3× as a 6-helix tube. The dimer band in lane 2 (4-row cyclization units at 2×) ran as fast as the monomer band in lane 4 (8-row cyclization units at 1×), confirming the 4-row cyclization unit multimerizes at 2× as an 8-helix tube. Same correspondence between the dimer band in lane 3 (6-row cyclization units at 2×) and the monomer band in lane 5 (12-row cyclization units at 1×). Corresponding TEM images and detailed examples are shown in Figures S10-S22. Lane 6: 1-kb ladder.

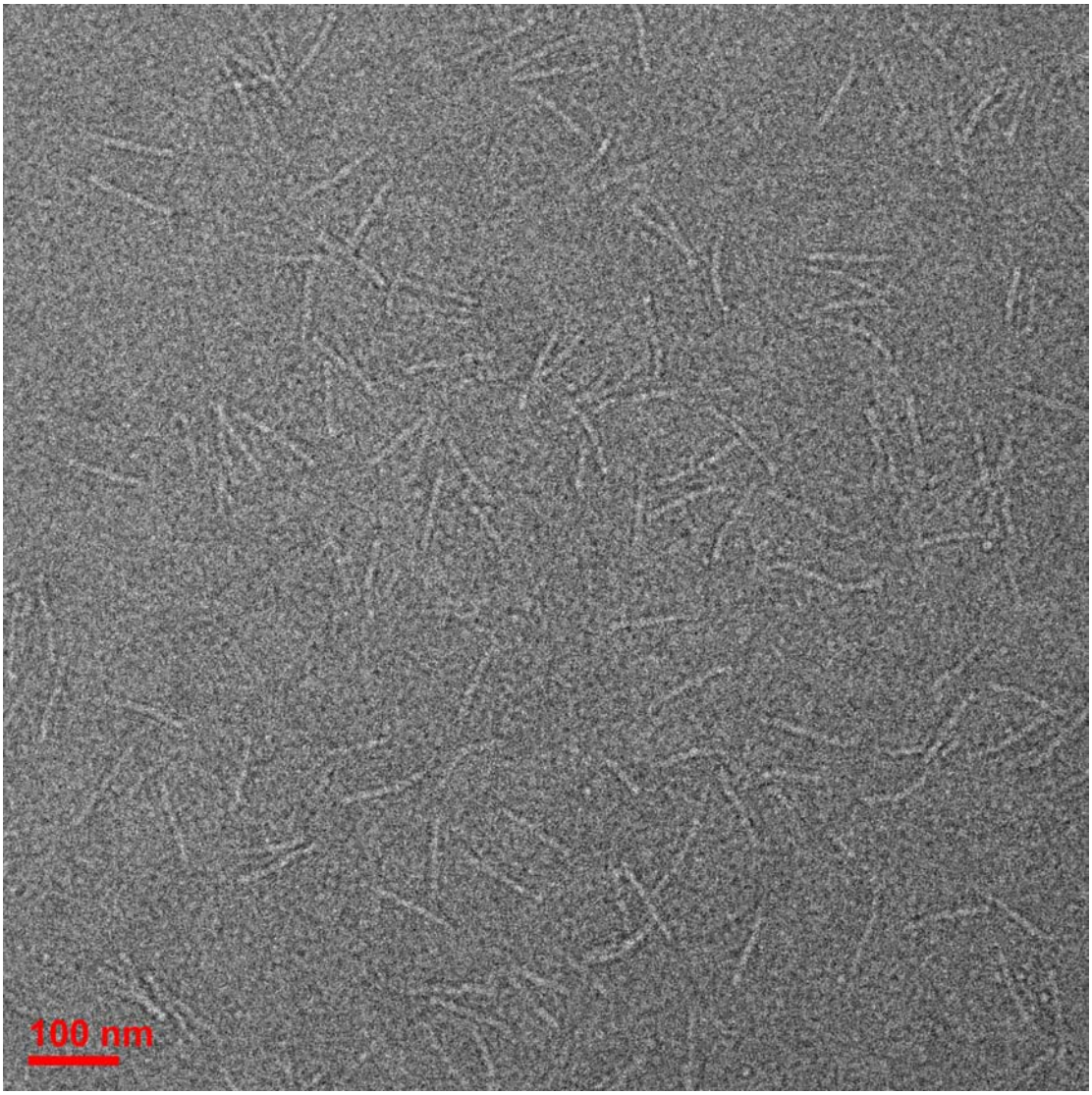

Figure S10. TEM image of tubes from the 2-row cyclization unit of U2-SSTs directly after self-assembly without purification. Scale bar: 100 nm.

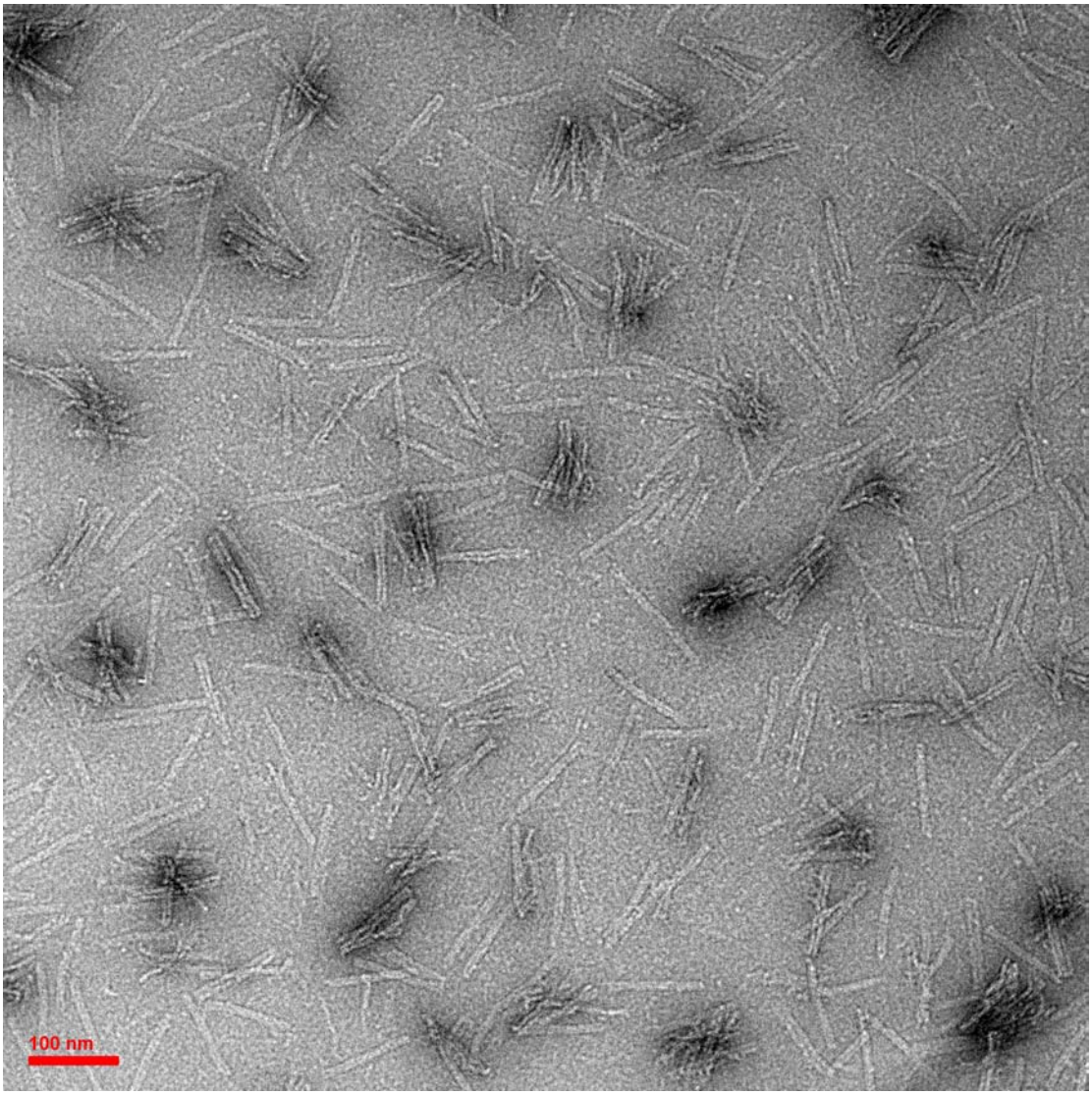

Figure S11. TEM image of tubes from the 4-row cyclization unit of U2-SSTs directly after self-assembly without purification. Scale bar: 100 nm.

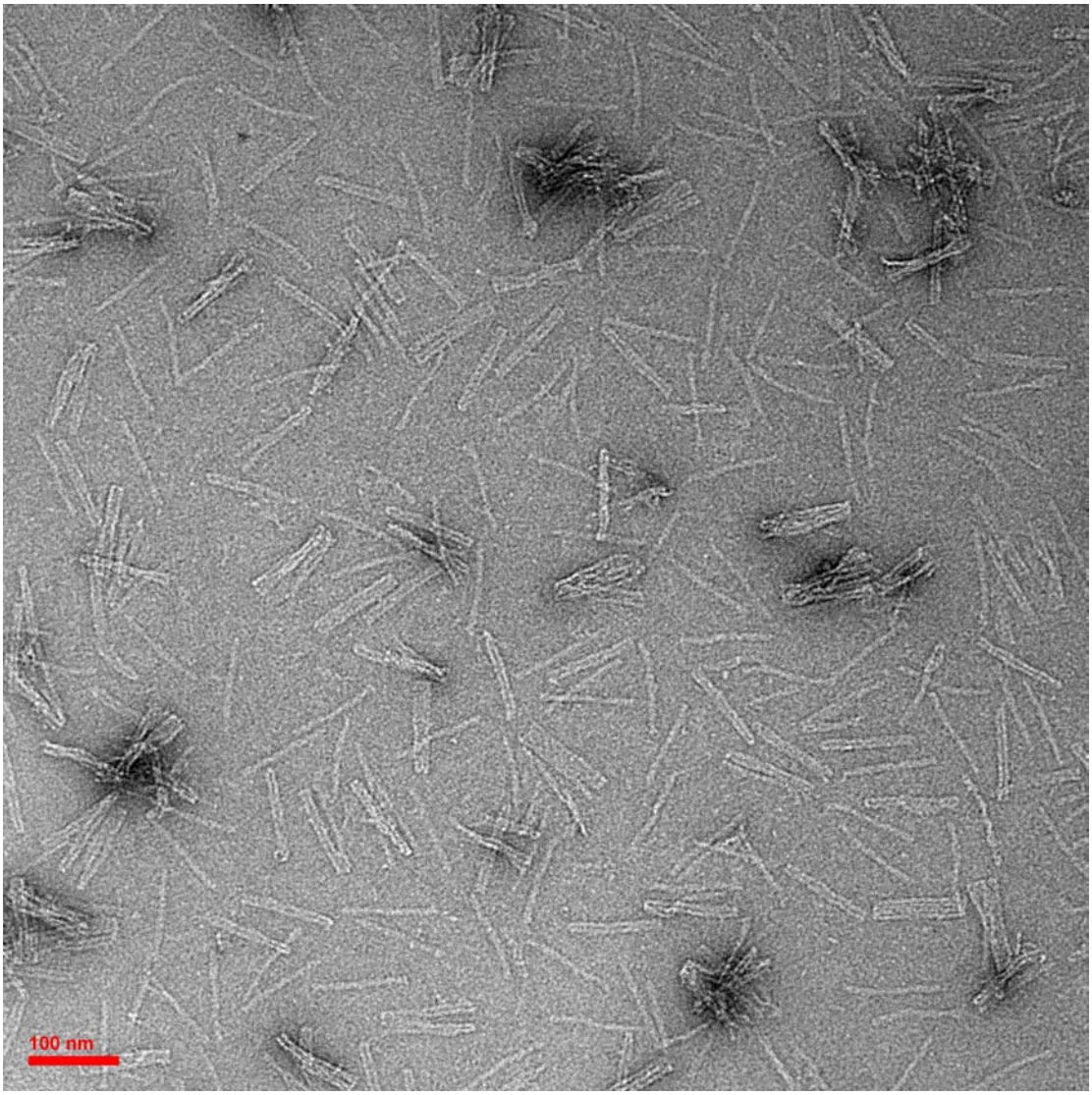

Figure S12. TEM image of tubes from the 6-row cyclization unit of U2-SSTs directly after self-assembly without purification. Scale bar: 100 nm.

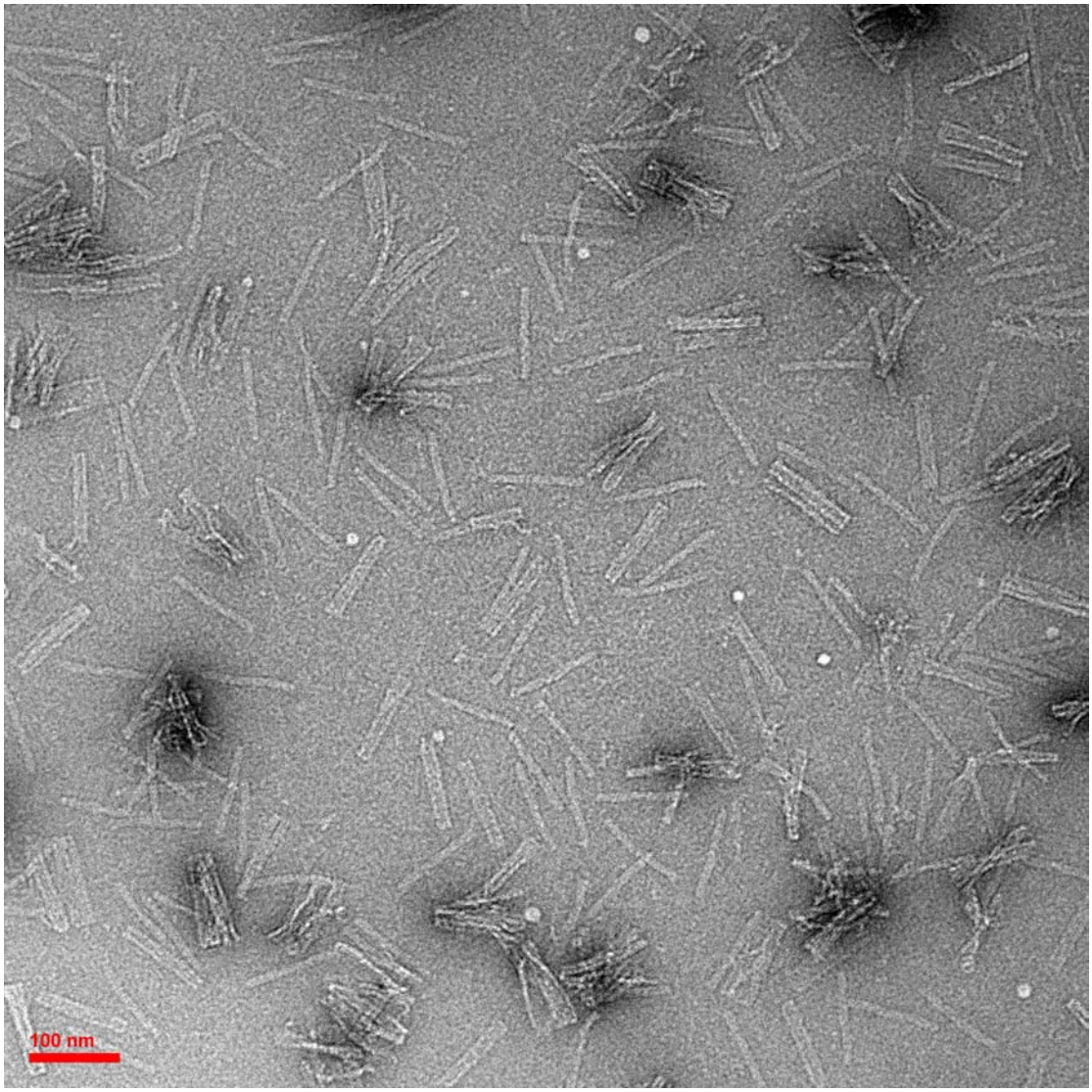

Figure S13. TEM image of tubes from the 8-row cyclization unit of U2-SSTs directly after self-assembly without purification. Scale bar: 100 nm.

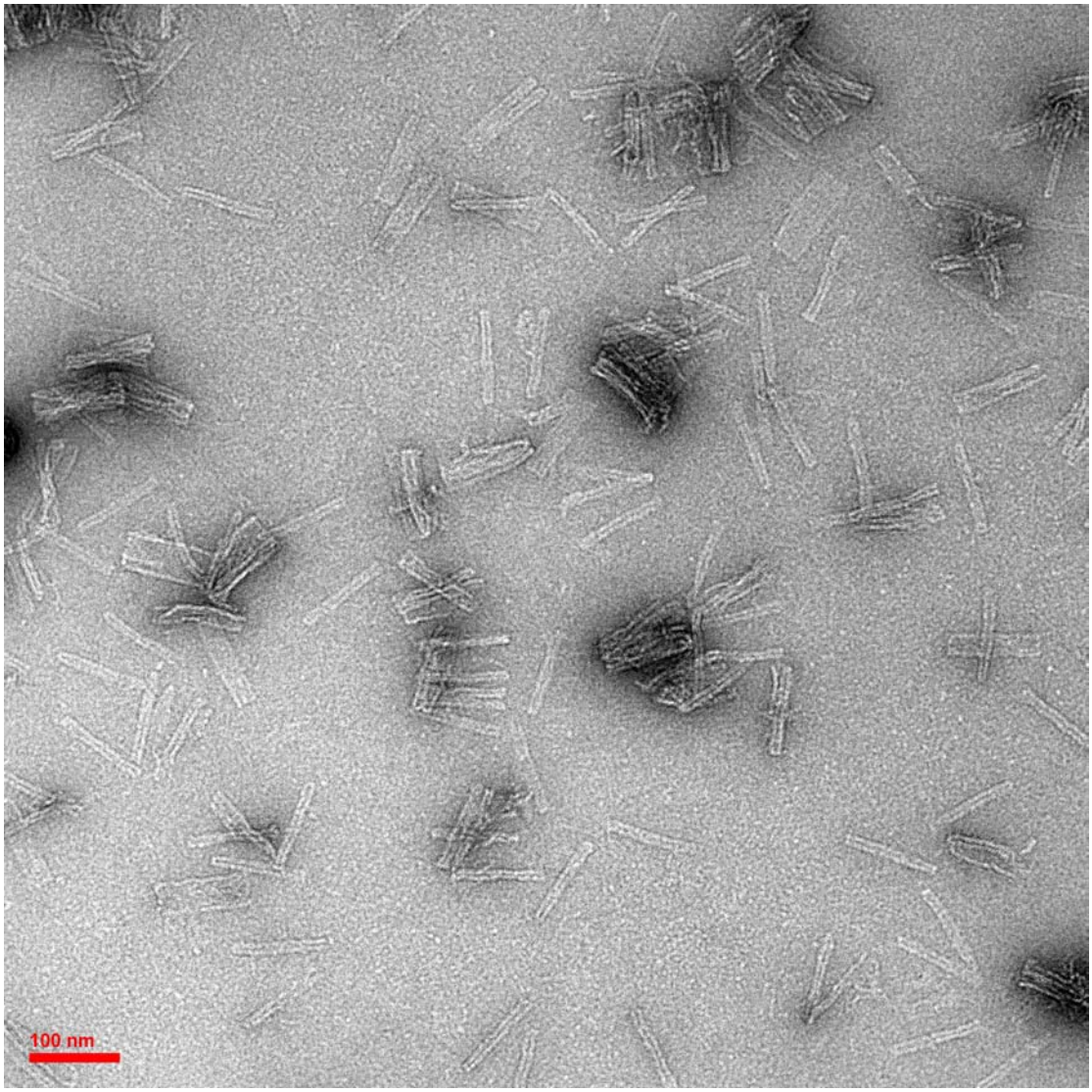

Figure S14. TEM image of tubes from the 12-row cyclization unit of U2-SSTs directly after self-assembly without purification. Scale bar: 100 nm.

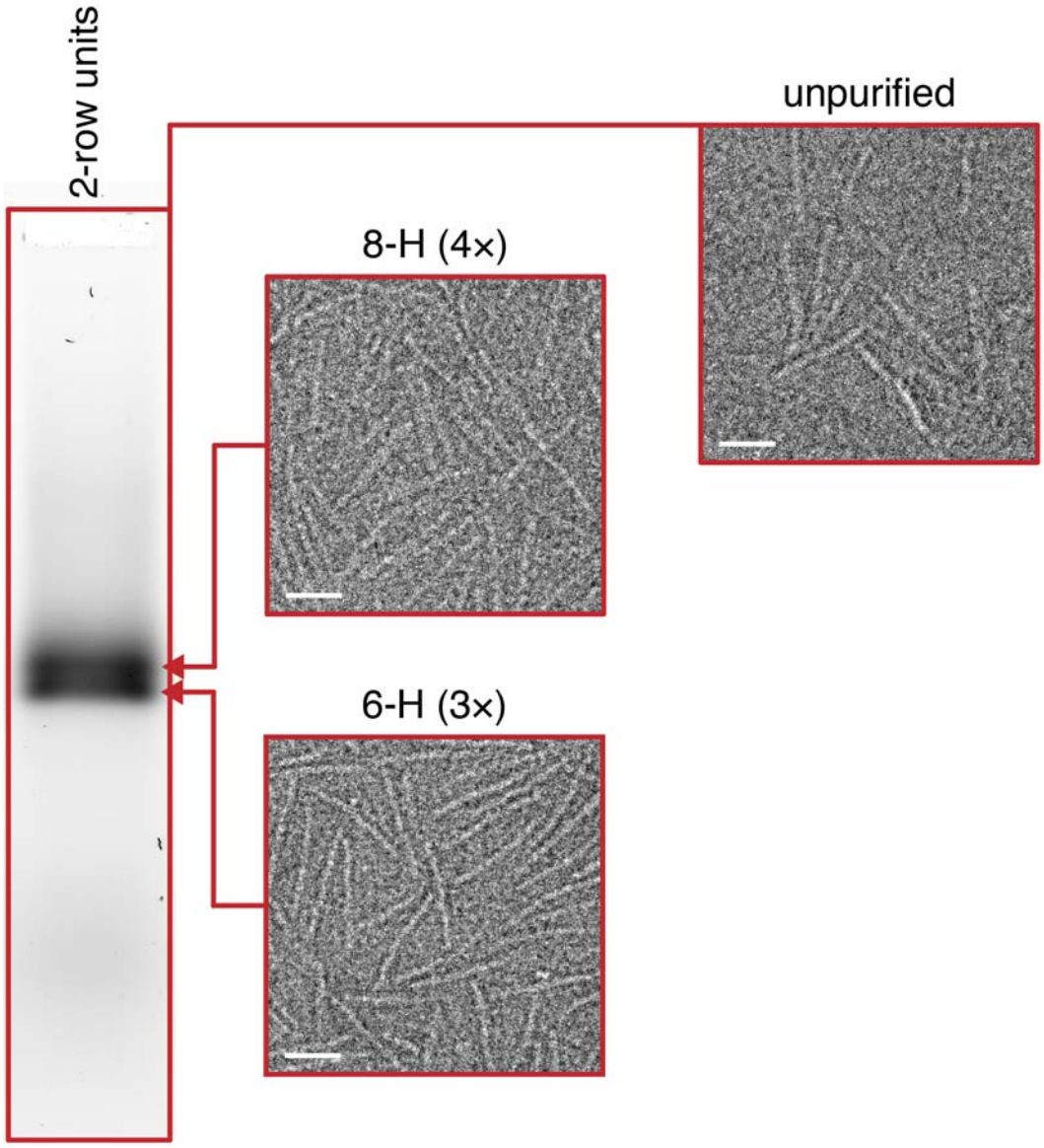

Figure S15. AGE and TEM results of the 2-row cyclization unit of U2-SSTs at different repetitive levels. AGE results are shown on the left. Products of 2-row units multimerizing at 3× (6-H) and 4× (8-H) are pointed by triangles. The rectangle framing the whole lane depicts the product after self-assembly without purification. Corresponding TEM images are presented on the right. Scale bars: 50 nm.

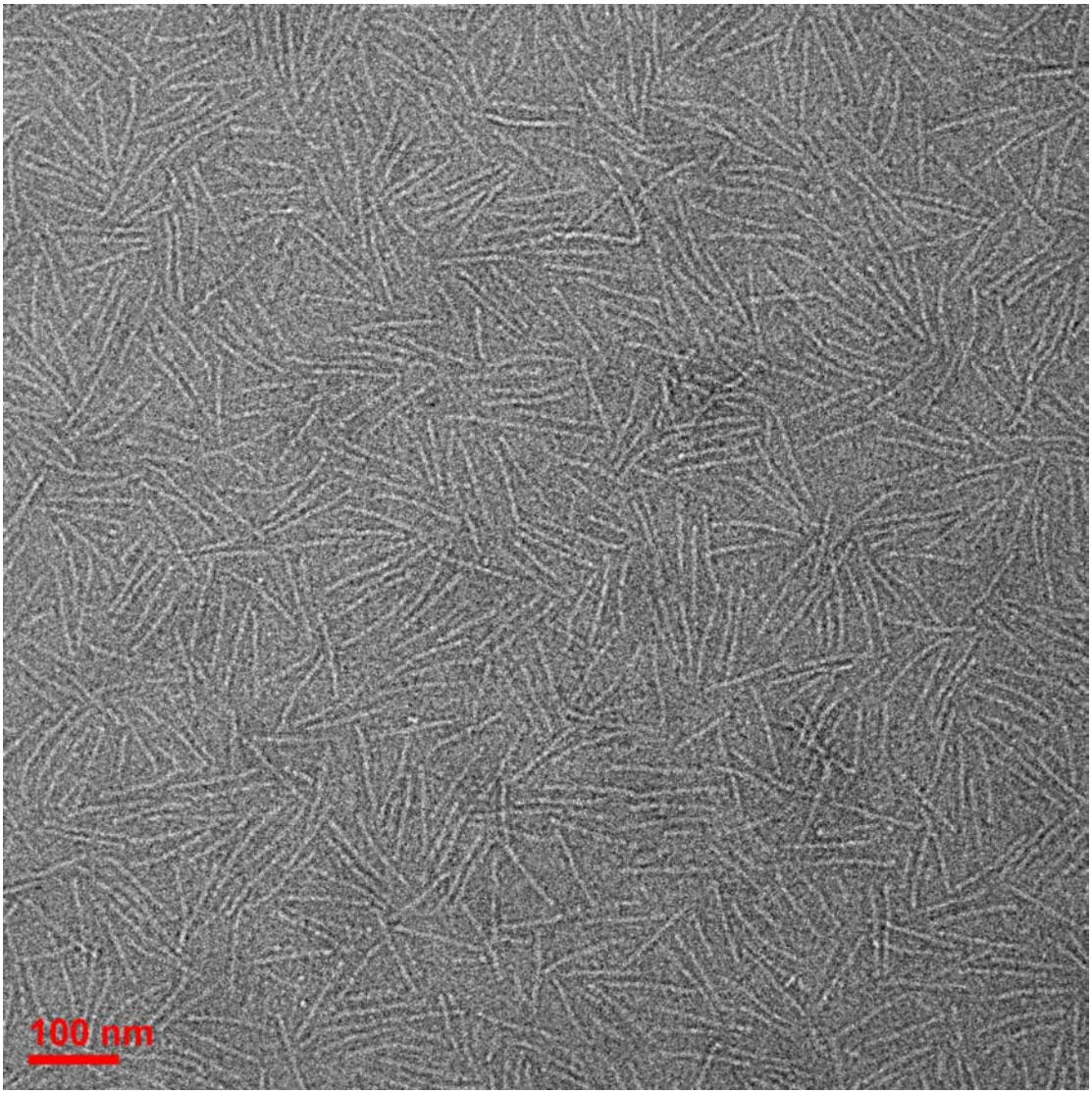

Figure S16. TEM image of tubes from the 2-row cyclization unit of U2-SSTs multimerizing at 3× (the trimer band of lane 1 in Figure S9) after purification. Scale bar: 100 nm. Width measurements are shown in Table S1.

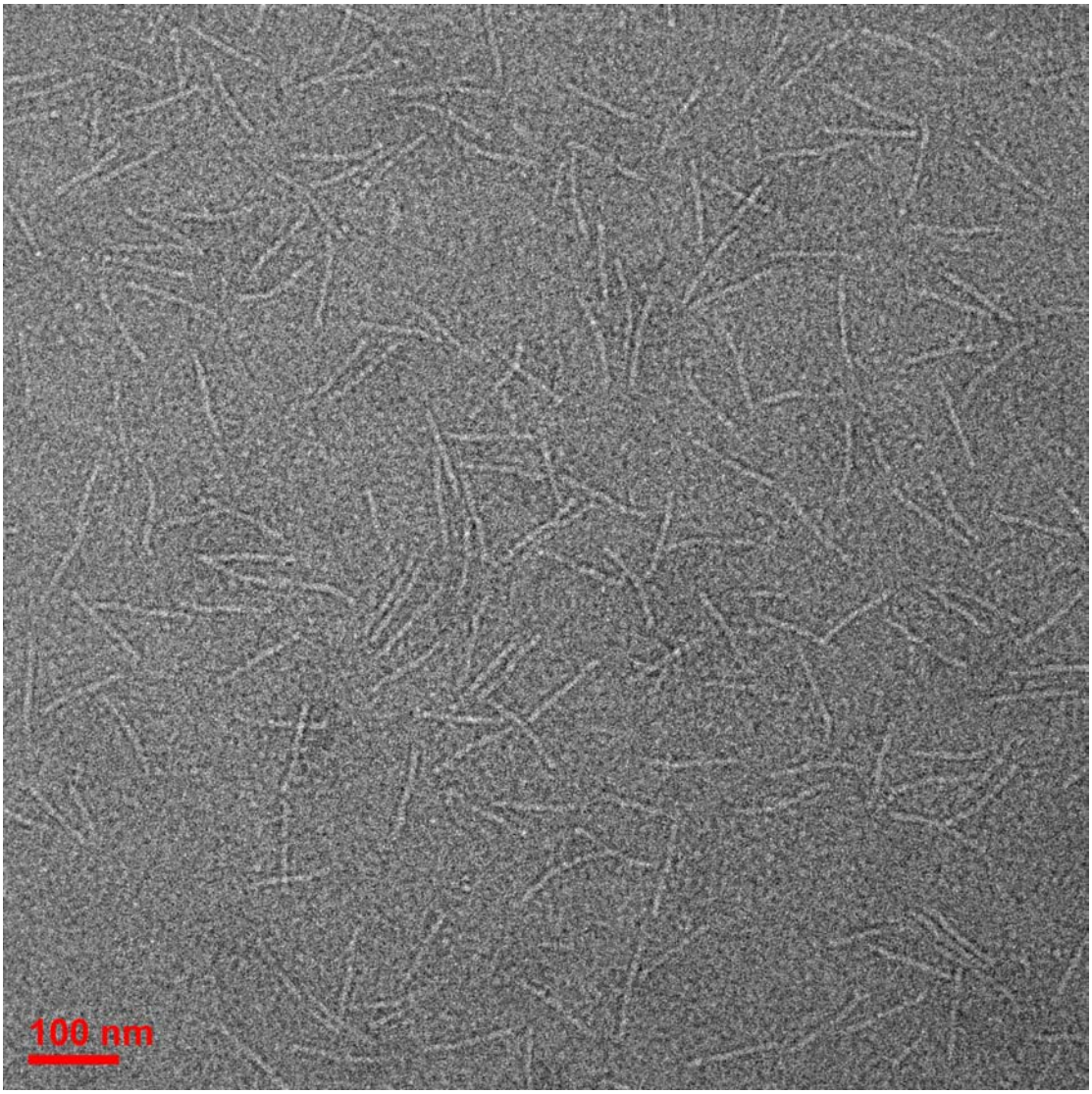

Figure S17. TEM image of monomer tubes from the 6-row cyclization unit of U2-SSTs (the monomer band of lane 3 in Figure S9) after purification as a comparison with tubes shown in Figure S16. Scale bar: 100 nm. Width measurements are shown in Table S1.

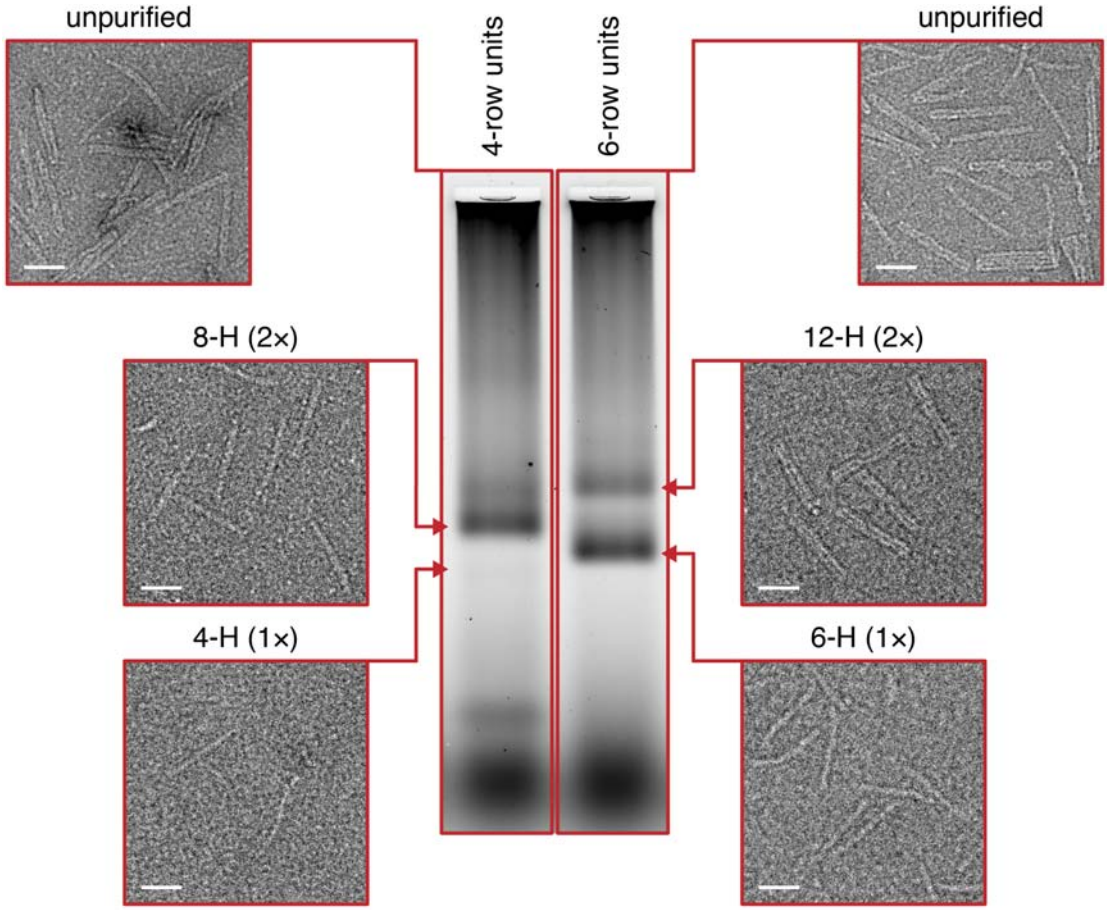

Figure S18. AGE and TEM results of the 4-row and 6-row cyclization units of U2-SSTs at different repetitive levels. AGE results are shown in the middle. Monomer (1×) and dimer (2×) products of cyclization units are pointed by triangles. The rectangles framing the whole lane depict the products after self-assembly without purification. Corresponding TEM images of 4-row and 6-row cyclization units are presented on the left and right respectively. Scale bars: 50 nm.

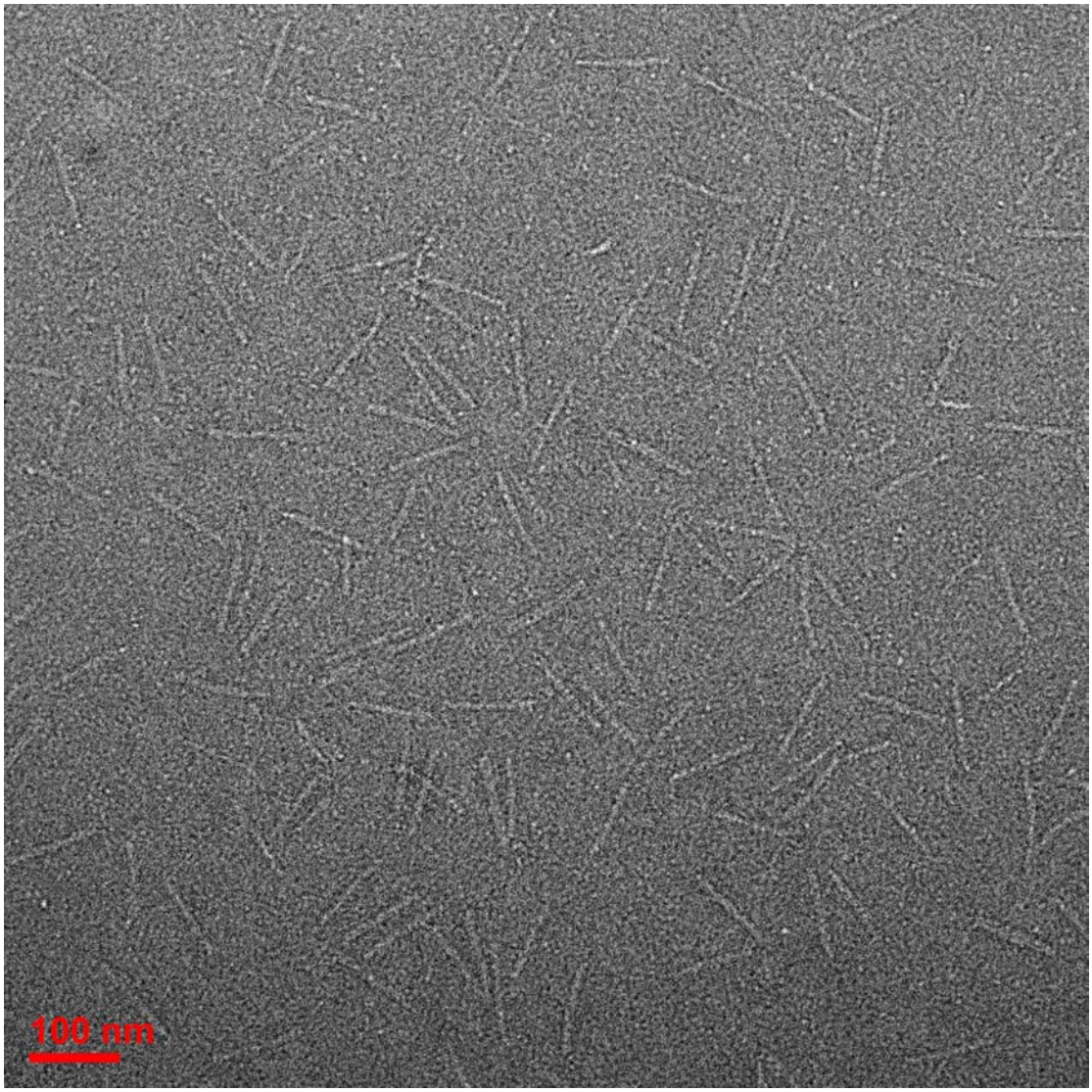

Figure S19. TEM image of tubes from the 4-row cyclization unit of U2-SSTs multimerizing at 2× (the dimer band of lane 2 in Figure S9) after purification. Scale bar: 100 nm. Width measurements are shown in Table S1.

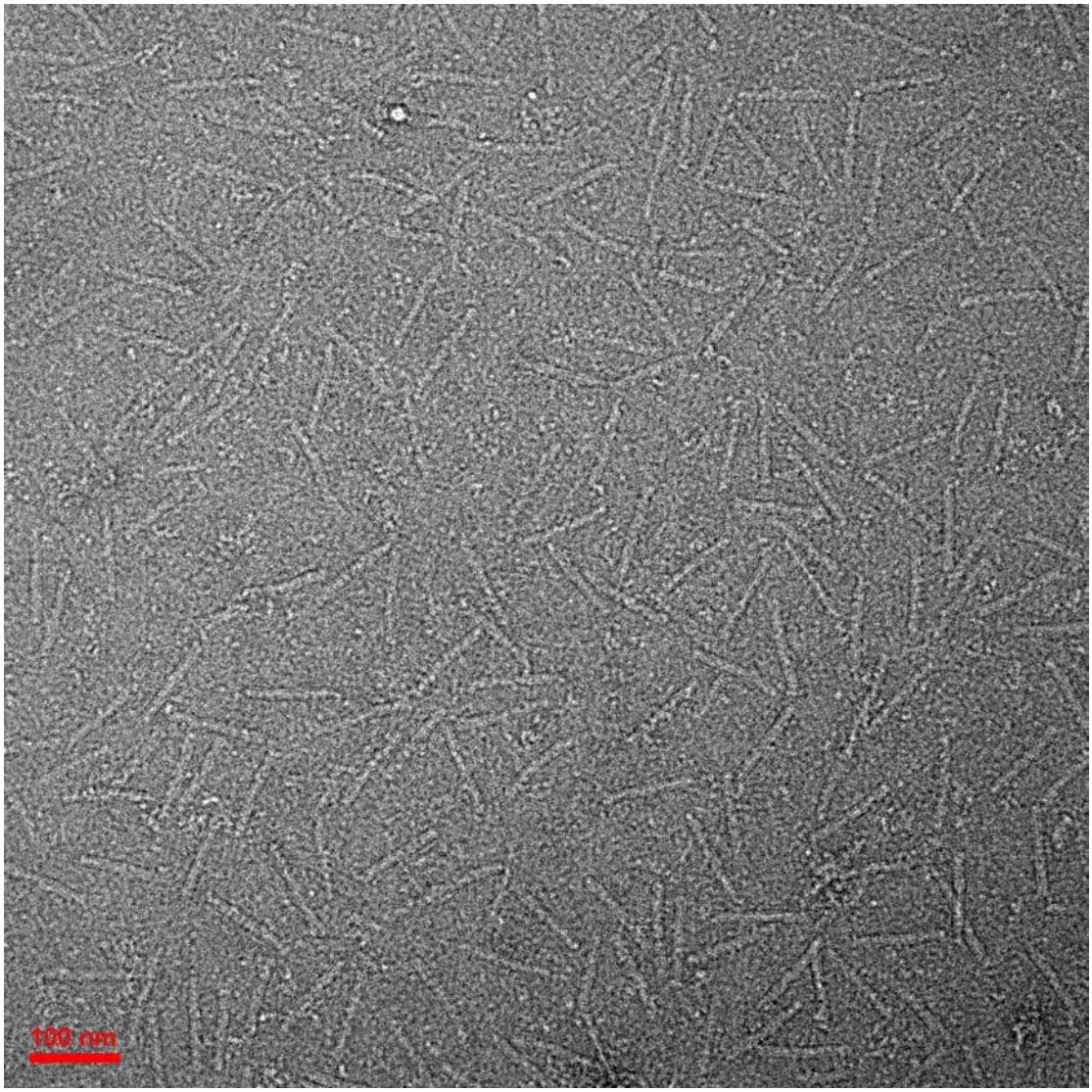

Figure S20. TEM image of monomer tubes from the 8-row cyclization unit of U2-SSTs (the monomer band of lane 4 in Figure S9) after purification as a comparison with tubes shown in Figure S19. Scale bar: 100 nm. Width measurements are shown in Table S1.

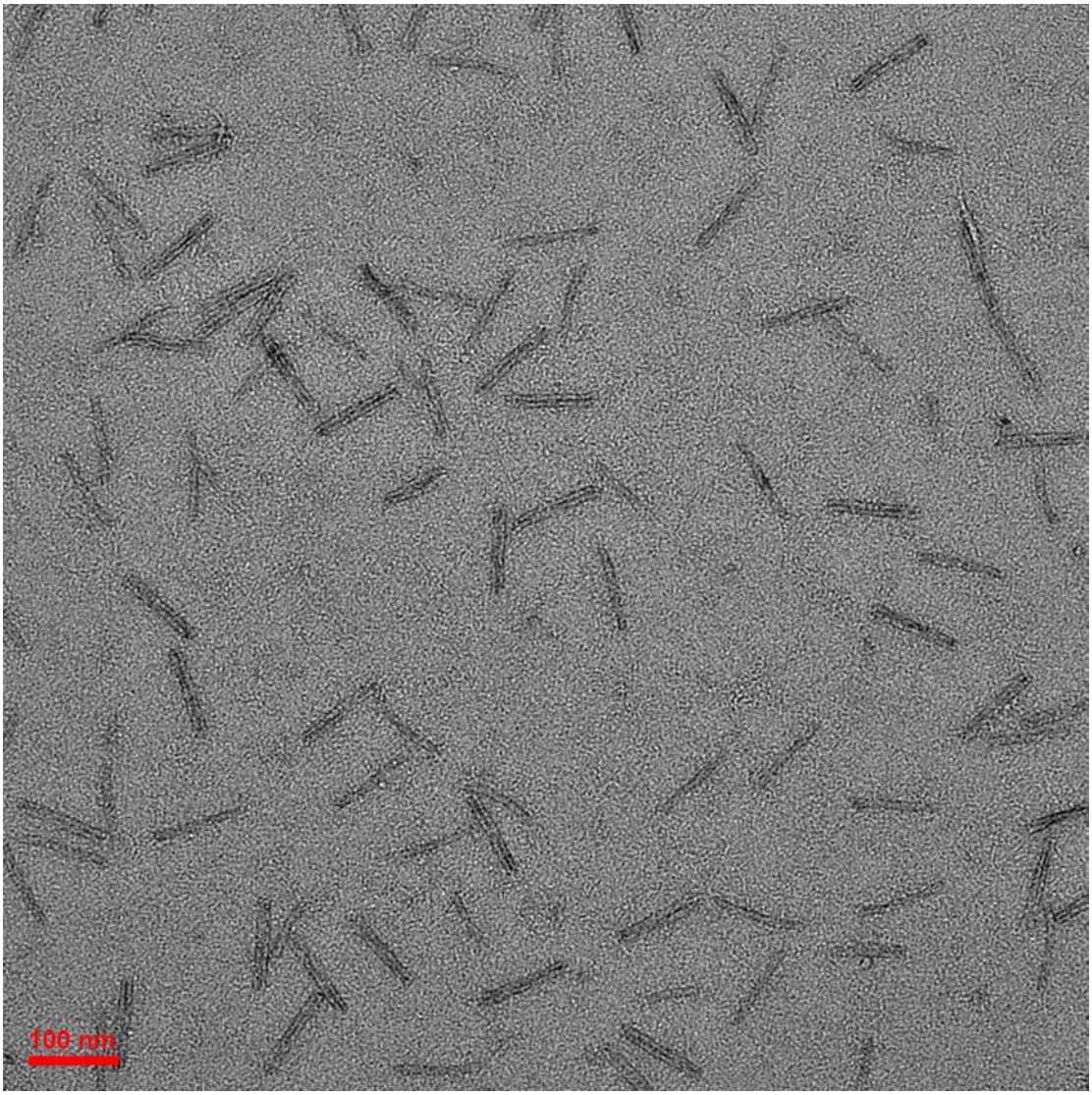

Figure S21. TEM image of tubes from the 6-row cyclization unit of U2-SSTs multimerizing at 2× (the dimer band of lane 3 in Figure S9) after purification. Scale bar: 100 nm. Width measurements are shown in Table S1.

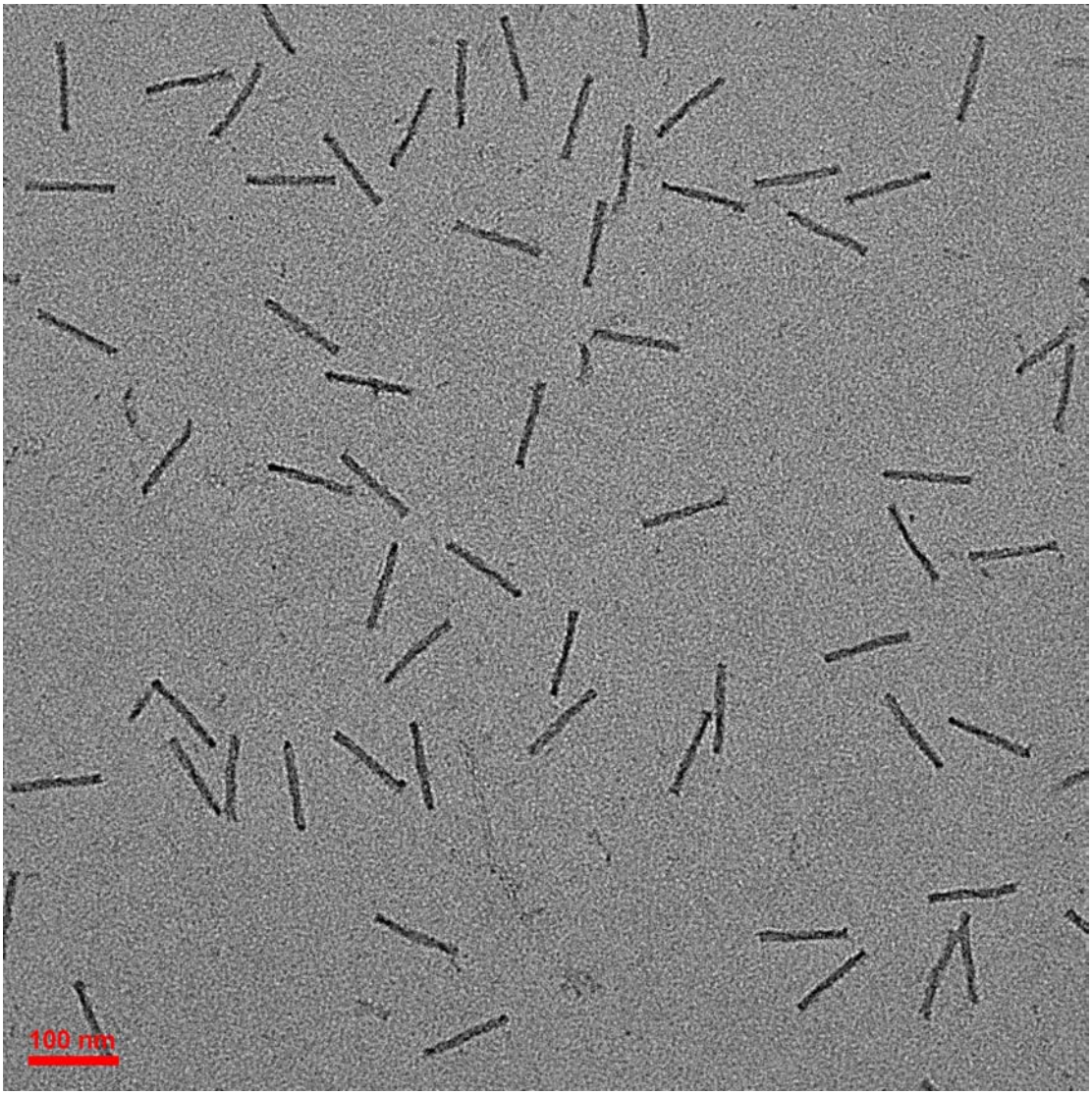

Figure S22. TEM image of monomer tubes from the 12-row cyclization unit of U2-SSTs (the monomer band of lane 5 in Figure S9) after purification as a comparison with tubes shown in Figure S21. Scale bar: 100 nm. Width measurements are shown in Table S1.

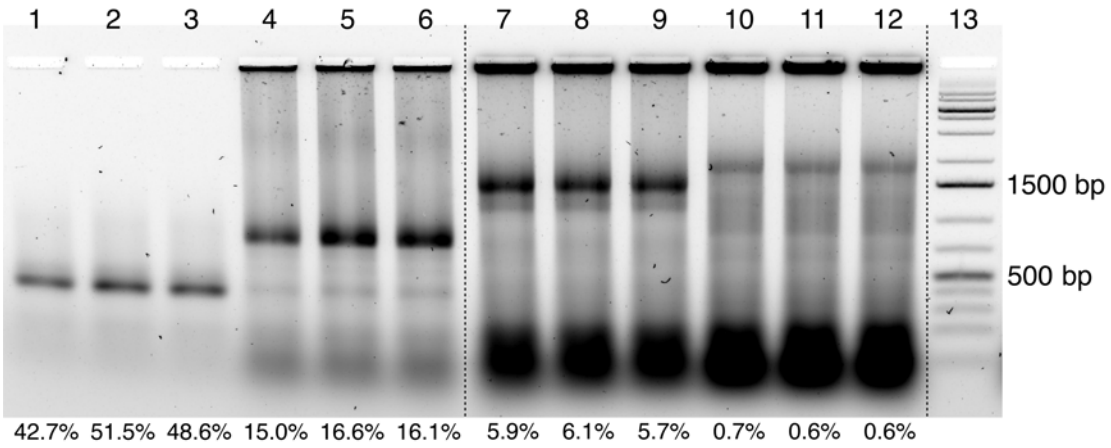

Figure S23. AGE results of 4-helix tubes (2× repetition) from 2-row cyclization units of U-SSTs with different numbers of addressable columns. Lane 1-3: tubes with 10 addressable columns. Lane 4-6: tubes with 30 addressable columns. Lane 7-9: tubes with 70 addressable columns. Lane 10-12: tubes with 100 addressable columns. Lane 13: 1-kb ladder. Percentages at the bottom indicate corresponding assembly yields of the tubes. Quantification method is introduced in Methods. Corresponding TEM images of purified products are shown in Figures S24-S27.

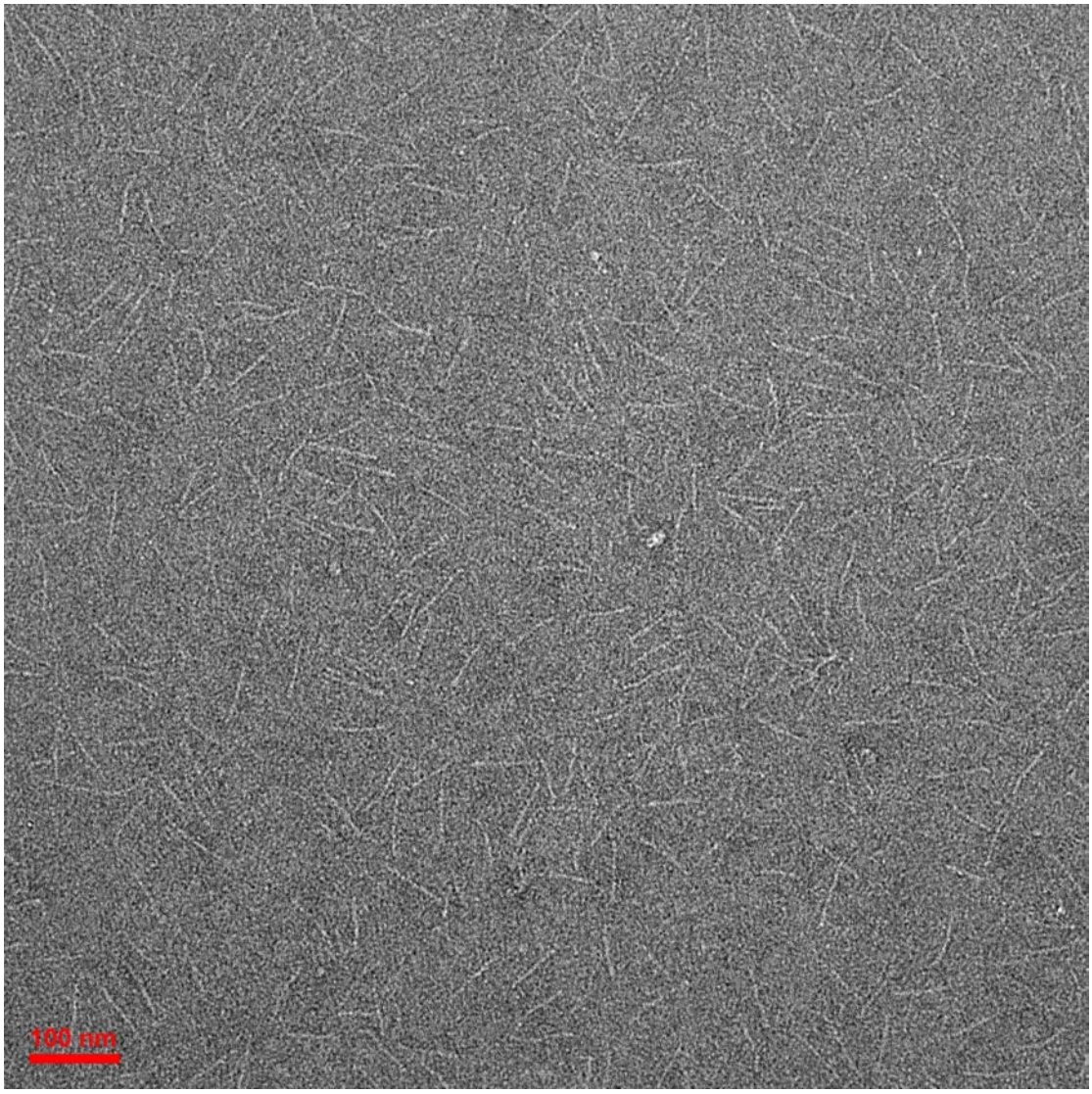

Figure S24. TEM image of 4-helix tubes (2× repetition) from 2-row cyclization units of U-SSTs with 10 addressable columns after purification. Scale bar: 100 nm. Length measurements are shown in Table S2.

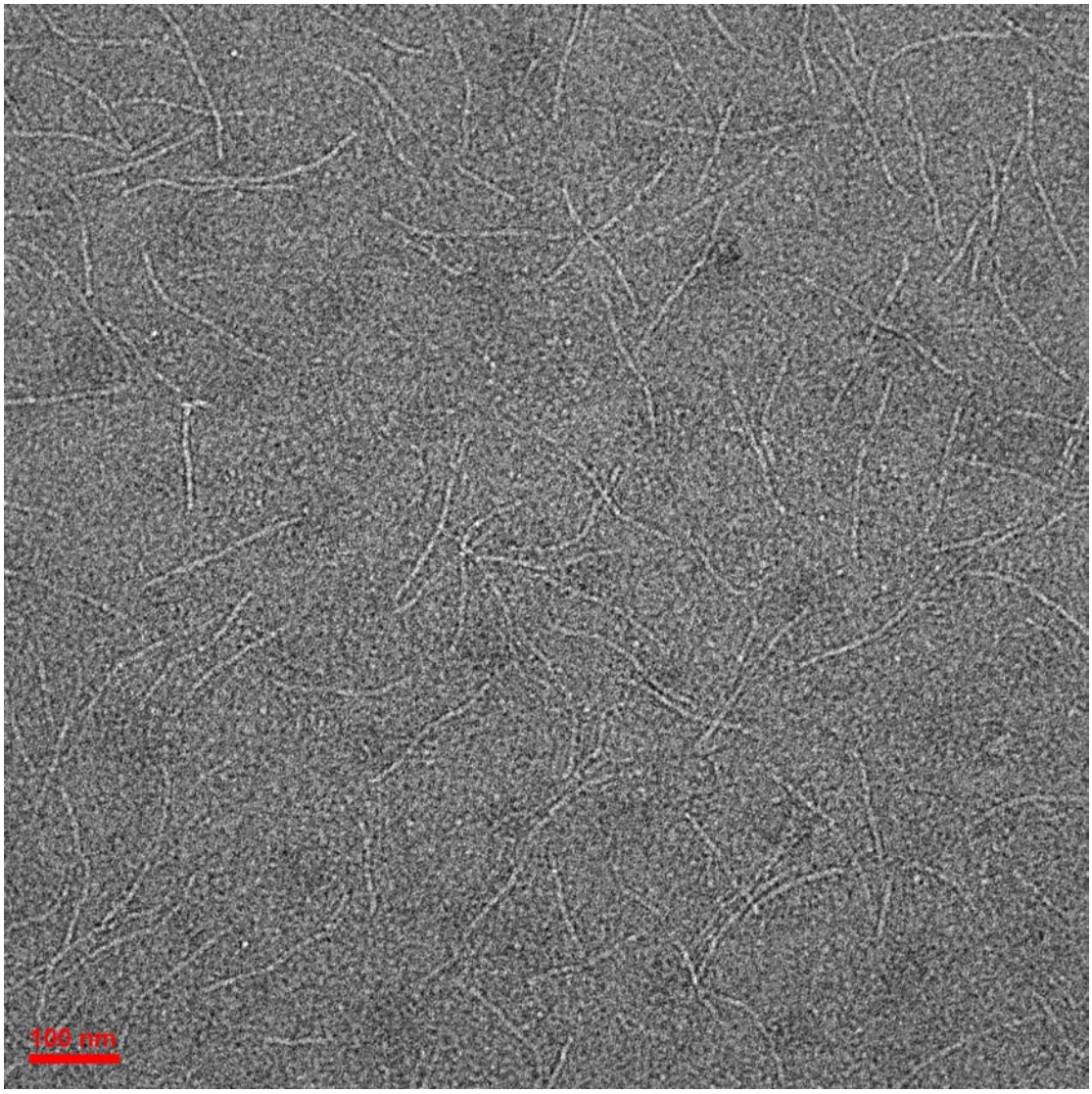

Figure S25. TEM image of 4-helix tubes (2× repetition) from 2-row cyclization units of U-SSTs with 30 addressable columns after purification. Scale bar: 100 nm. Length measurements are shown in Table S2.

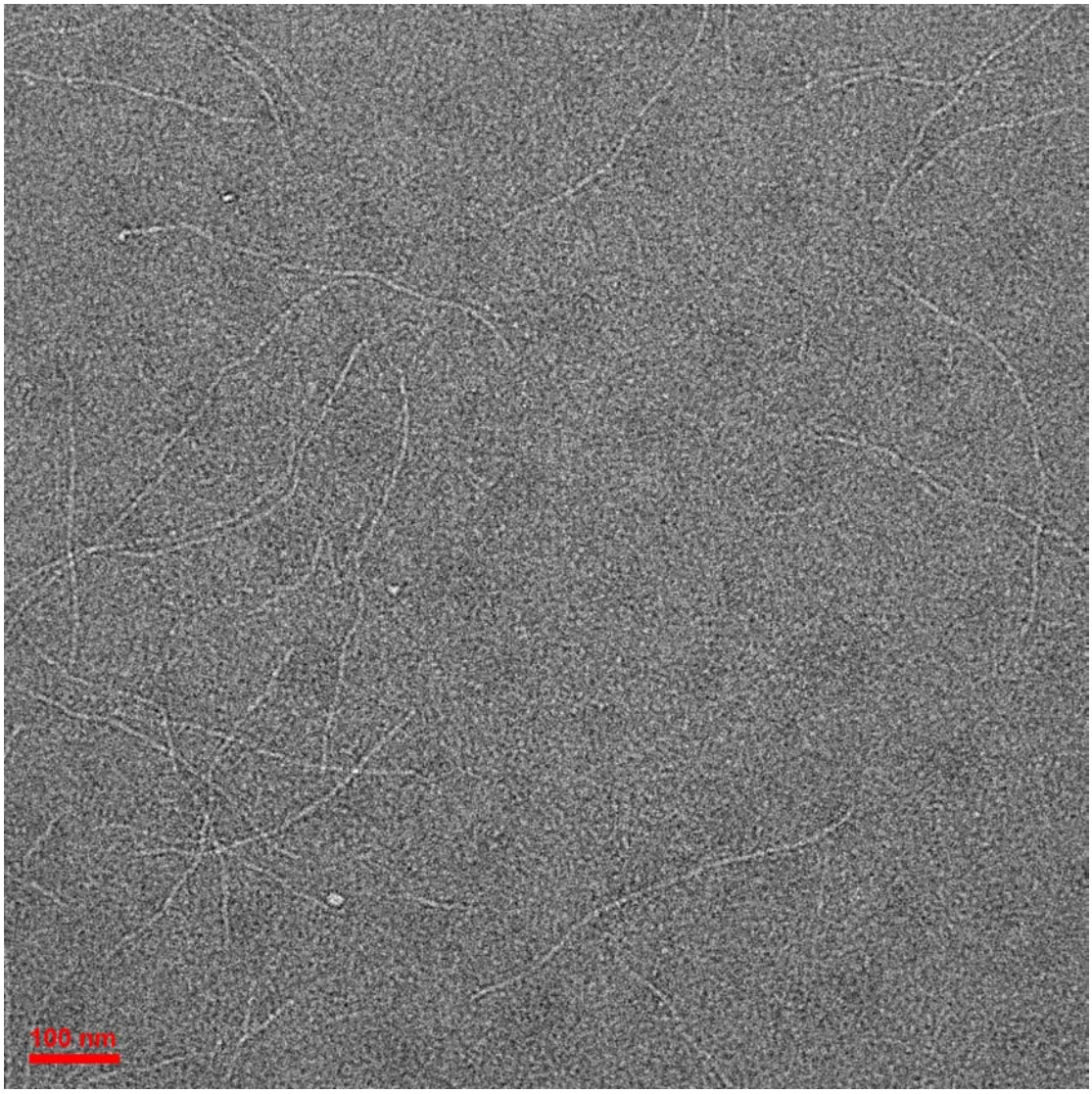

Figure S26. TEM image of 4-helix tubes (2× repetition) from 2-row cyclization units of U-SSTs with 70 addressable columns after purification. Scale bar: 100 nm. Length measurements are shown in Table S2.

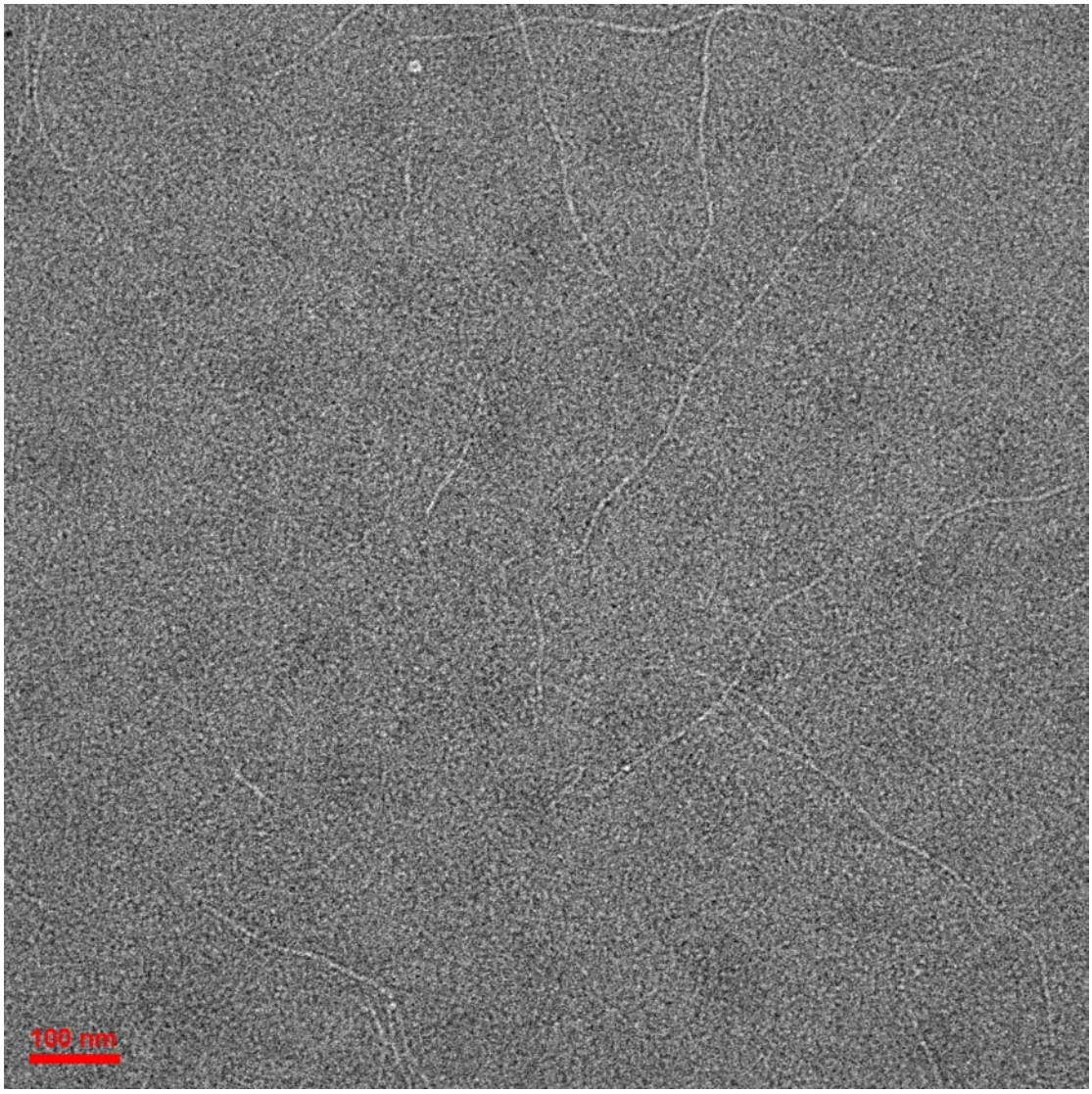

Figure S27. TEM image of 4-helix tubes (2× repetition) from 2-row cyclization units of U-SSTs with 100 addressable columns after purification. Scale bar: 100 nm. Length measurements are shown in Table S2.

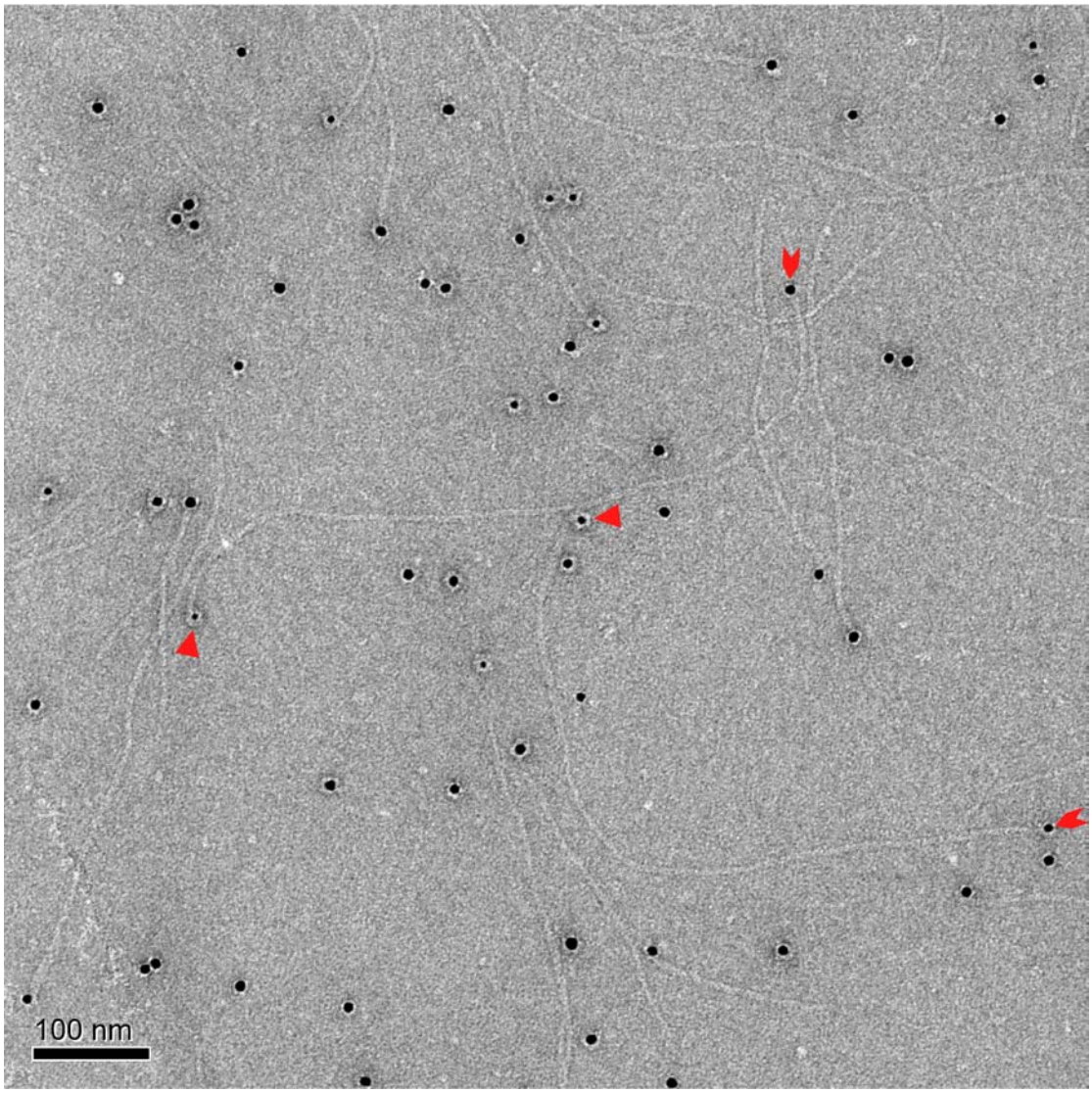

Figure S28. TEM image of 100-column tubes from 2-row cyclization units of U-SSTs with AuNPs decoration. The leftmost and rightmost tiles of the 100-column tube were pre-conjugated with 10-nm (chevrons) and 5-nm (triangles) AuNPs respectively. Some tubes were half-decorated or without decoration due to the limited decoration efficiency of AuNPs and the fragility of the purified tubes. Scale bar: 100 nm.

Notes: Persistence length of tubular structures along the lateral direction

We estimated the persistence length of the tubular structures along the lateral direction based on a worm-like chain model[7]. The persistence length a of a worm-like chain model is defined by

$$a = \frac{l}{1 - \cos\alpha}$$

where α is the angle between adjacent vectors and l is the length of a unit. In this case, the angle equals to the average curvature of a tube and the length corresponds to the diameter of a double helix (~2.3 nm)[2]. Based on the multimerization results of tubes from 2-row cyclization units, the resulted products from 2-row units of U-SSTs and U2-SSTs are 4-helix and 6-helix tubes, whose average curvatures are 90° and 60° respectively. Therefore, the persistence length of U-shaped SSTs was calculated as 2.3~5 nm (l=2.3 nm; α=90° or 60°).

Table S1. Width measurements of tubes from different types of SSTs.

Structure		Width (nm)
U-SSTs	2-row units at 2× (N = 168)	7.8 ± 0.9
	4-row units at 1× (N = 206)	7.6 ± 1.4
	6-row units at 1× (N = 163)	10.6 ± 1.4
	12-row units at 1× (N = 85)	17.8 ± 1.5
	24-row units at 1× (N = 68)	25.4 ± 1.9
U2-SSTs	2-row units at 3× (N = 77)	8.1 ± 0.7
	4-row units at 2× (N = 102)	9.3 ± 1.2
	6-row units at 1× (N = 127)	8.4 ± 1.3
	6-row units at 2× (N = 104)	12.5 ± 1.6
	8-row units at 1× (N = 105)	10.9 ± 1.3
	12-row units at 1× (N = 118)	11.6 ± 1.5

Table S2. Assembly yield quantification and length measurements of tubes with addressable columns from 2-row cyclization units of U-SSTs.

Structure	Assembly yield (mean ± SD, N=3)	Length (nm) (mean±SD)
10-column	47.6% ± 4.4%	70.7 ± 8.7 (N = 106)
30-column	15.9% ± 0.8%	204.2 ± 10.7 (N = 108)
70-column	5.9% ± 0.2%	472.1 ± 25.2 (N = 113)
100-column	0.6% ± 0.1%	662.3 ± 33.1 (N = 34)

References

1 Wei, B., Dai, M. & Yin, P. Complex Shapes Self-Assembled from Single-Stranded DNA Tiles. *Nature* **485**, 623 (2012).

2 Wei, B. *et al.* Design Space for Complex DNA Structures. *J. Am. Chem. Soc.* **135**, 18080 (2013).

3 Wei, B., Wang, Z. & Mi, Y. Uniquimer: Software of De Novo DNA Sequence Generation for DNA Self-Assembly—An Introduction and the Related Applications in DNA Self-Assembly. *Journal of Computational and Theoretical Nanoscience* **4**, 133-141, doi:10.1166/jctn.2007.013 (2007).

4 Sharma, J., Chhabra, R., Liu, Y., Ke, Y. & Yan, H. DNA-Templated Self-Assembly of Two-Dimensional and Periodical Gold Nanoparticle Arrays. *Angew. Chem., Int. Ed.* **45**, 730 (2006).

5 Sharma, J. *et al.* Toward Reliable Gold Nanoparticle Patterning on Self-Assembled DNA Nanoscaffold. *J. Am. Chem. Soc.* **130**, 7820 (2008).

6 Sun, W. *et al.* Casting inorganic Structures with DNA Molds. *Science* **346**, 1258361 (2014).

7 Geoghegan, M. & Hadziioannou, G. *Polymer Electronics*. (OUP Oxford, 2013).